Goodman, R. E. (1995). *Géotechnique* **45**, No. 3, 383–423

Block theory and its application

R. E. GOODMAN*

Block theory is a geometrically based set of analyses that determine where potentially dangerous blocks can exist in a geological material intersected by variously oriented discontinuities in three dimensions. It applies ideally to hard, blocky rock in which blocks of various sizes may be potential sources of load and hazard in an excavation or foundation. Block theory also can apply to rocks that are highly porous, weathered and fissured, and it may have applicability to some soils. The lecture discusses problems faced in attempting to characterize blocky rock and reviews some methods for gaining adequate data about joint systems. The underlying assumptions of block theory are examined in relation to recent developments and refinements. The main ideas of block theory are reviewed, as are their application to finding and describing key-blocks of tunnels, slopes and foundations. Both translational and rotational analysis are covered, the latter being a recent enlargement of block theory. Examples of practical problems that can be solved using block theory are identifying and analysing problems of safety posed by actual blocks in foundations of existing dams, finding design blocks for laying out and selecting supports for tunnels in complexly jointed rock masses, finding the minimum safe thickness of a pillar between parallel excavations, estimating real key-block regions for tunnels of different size in joint systems that are not infinitely long, and finding the optimal directions for tunnelling or shafting through a rock mass. Some illustrative cases are introduced.

KEYWORDS: anisotropy; geology; numerical modelling and analysis; rocks/rock mechanics; slopes; tunnels.

La théorie des blocs est un ensemble d'analyses géométriques permettant de localiser les blocs potentiellement dangereux dans un matériau géologique recoupé dans les trois dimensions par les discontinuités d'orientations variables. Elle s'applique idéalement aux roches dures pour lesquelles des blocs de tailles diverses peuvent être sources potentielles de charge et de risque lors d'une excavation ou d'une fondation. La théorie des blocs est également applicable aux roches fortement poreuses, altérées et fissurées, ainsi qu'à certains sols. La conférence s'intéresse aux problèmes recontrés lors des tentatives de caractérisation des roches à blocs et passe en revue quelques méthodes permettant d'obtenir des données adaptées aux systèmes de joints. Les hypothèses fondamentales de la théorie des blocs sont étudiées au travers des développements et perfectionnements récents. Les idées de base de cette théorie, et leurs applications à la découverte et à la description des blocs-clés des tunnels, talus et fondations, sont examinées. On évoquera les analyses translationnelles et les analyses rotationnelles, ces dernières correspondant à un élargissement récent de la théorie des blocs. Les problèmes pratiques pouvant être résolus à l'aide de la théorie des blocs sont typiquement: identifier et analyser les problèmes de sûreté dus à des blocs récents sur les fondations de barrages préexistants; trouver un design de blocs permettant de sélectionner et de poser le soutènement dans des tunnels creusés dans des masses rocheuses à joints complexes; calculer l'épaisseur de sécurité minimale pour un pieu situé entre deux excavations parallèles; estimer, dans un tunnel, les régions réelles de blocs-clés pour des systèmes de joints de différentes tailles mais de longueur finie; et trouver les directions optimales de creusement dans une masse rocheuse. Quelques cas types sont présentés.

This is a unique opportunity to invest in an examination of block theory and its application to engineering for excavations in rock. It may be called a geometric approach, in contrast to one which dwells primarily on some sort of mathematical modelling based on the laws of continuum mechanics. A geometric solution is appropriate if the creation of an excavation is viewed as the introduction of a geometric space next to a rock mass; block theory evaluates the possibilities for the rock mass to invade this space. The method was introduced by Goodman & Shi (1985) who built on ideas initiated earlier by Shi in China when he—a topologist—was forced by political circumstances to perform manual labour underground in a hazardous excavation.

Charged with responsibility for design, an engineer hopes to have available tools appropriate to

* Cahill Professor of Geotechnical Engineering, University of California.

the applicable materials and conditions. When the materials are natural rock the only thing known with certainty is that this material will never be known with certainty. The deformability and strength of the different rock mass components, the distribution of water pressures and the in situ states of stress will, at best, be imperfectly understood. However, the internal structure and morphology of the bedrock units can often be discerned with greater confidence because the sciences of geology and geophysics are most effective in filling out this aspect of a site model. From a mechanical point of view, the engineering work together with the rock morphology will constitute a fully three-dimensional system.

The methods available to the engineer to evaluate design options in this rock system include empirical approaches that rely on previous experiences in similar classes of rock, special numerical model approaches tailored to the specific problem, analytical frameworks like block theory set up to work primarily with attainable structural details of the rock mass, and other methods adapted from continuum mechanics and which, in some cases, cannot be used without a great deal of judgement or even guesswork to bridge big gaps in required input information.

It may happen that the structural engineer is unaware how little the geotechnical engineer knows about the properties of a site; this leads to design by blind chance. This was a favourite theme of Karl Terzaghi (1960)

> Since few geologists are at home in the fields of mechanics and hydraulics, they commonly overestimate the amount of significant information one can derive even from a painstaking geological survey . . . I always make my decision, in connection with rock abutments, on the basis of the most unfavorable possibilities, compatible with what the survey has produced. In 1930 I prevented the construction of an arch dam in the eastern Caucasus at a site which was much more favorable than that of the Malpasset dam. However, if this reasoning were universally practiced, four out of five of the existing arch dams . . . would have never been built.

As many engineers do not practise this degree of conservatism, it seems there is an anti-Murphy's law—if something can go wrong, it probably won't—operating in matters of rock stability. This seems a doubtful premise for engineering. It would be better to calculate the implications of pessimistic assumptions for rock structure that are not incompatible with the results of the geotechnical survey. Block theory provides a means of doing this.

Block theory was developed to provide a theoretical basis for decision-making with reference to excavation layout and the design of supports in blocky rock. It requires knowledge of three-dimensional geologic structure and asks for only minimal data concerning the mechanical properties of the rock mass, namely the friction angles for the joints. The methods of block theory are generally inapplicable in non-blocky rock. In order to establish a context, some of the different classes of rock are now surveyed.

SOME TYPES OF ROCK MASS

The usual rock classifications of geology pertain to rock specimens and not to the structured rock masses encountered in a construction site. From a structural and mechanical point of view, nine classes of rock mass can be recognized.

(*a*) *Jointless rock* is found in many rock masses below the zone of weathering as, for example, massive sandstone, granitic rocks (Fig. 1(a)) and non-foliated basement rocks. The ideal analytical construct CHILE material* (continuous, homogeneous, isotropic and linearly elastic substance) may be approached in such rock masses.

(*b*) *Incompletely fractured rock* has fewer than three persistent joint sets so that, when excavated, the rock mass does not usually produce isolated blocks (Fig. 1(b)). Blockiness can be developed with the overlay of new fracturing in a direction not aligned with either pre-existing joint set. Methods of fracture mechanics are especially pertinent to computations in such rock masses. Non-convex excavations (e.g. those near pillars and where excavations intersect) can possibly produce blocks and block theory can be used to analyse these situations.

(*c*) *Incipiently blocky rock* has fewer than three joint sets open or filled with soils, but additional joint sets that are currently healed or tightly closed (Fig. 1(c)). The reawakening of one of these incipient joint sets, by strain, creates a real blocky condition. The likelihood of joints reopening can sometimes be studied using numerical modelling or mathematical analysis.

(*d*) *Blocky rock* has three or more persistent joint sets clearly developed and open or filled with soil that lacks appreciable tensile strength (Fig. 1(d)). The rock can be expected to produce blocks with a face in any excavated

* In numerous unpublished notes John Wade Bray of Imperial College (Royal School of Mines) referred to homogeneous, isotropic, linear elastic material as HILE material.

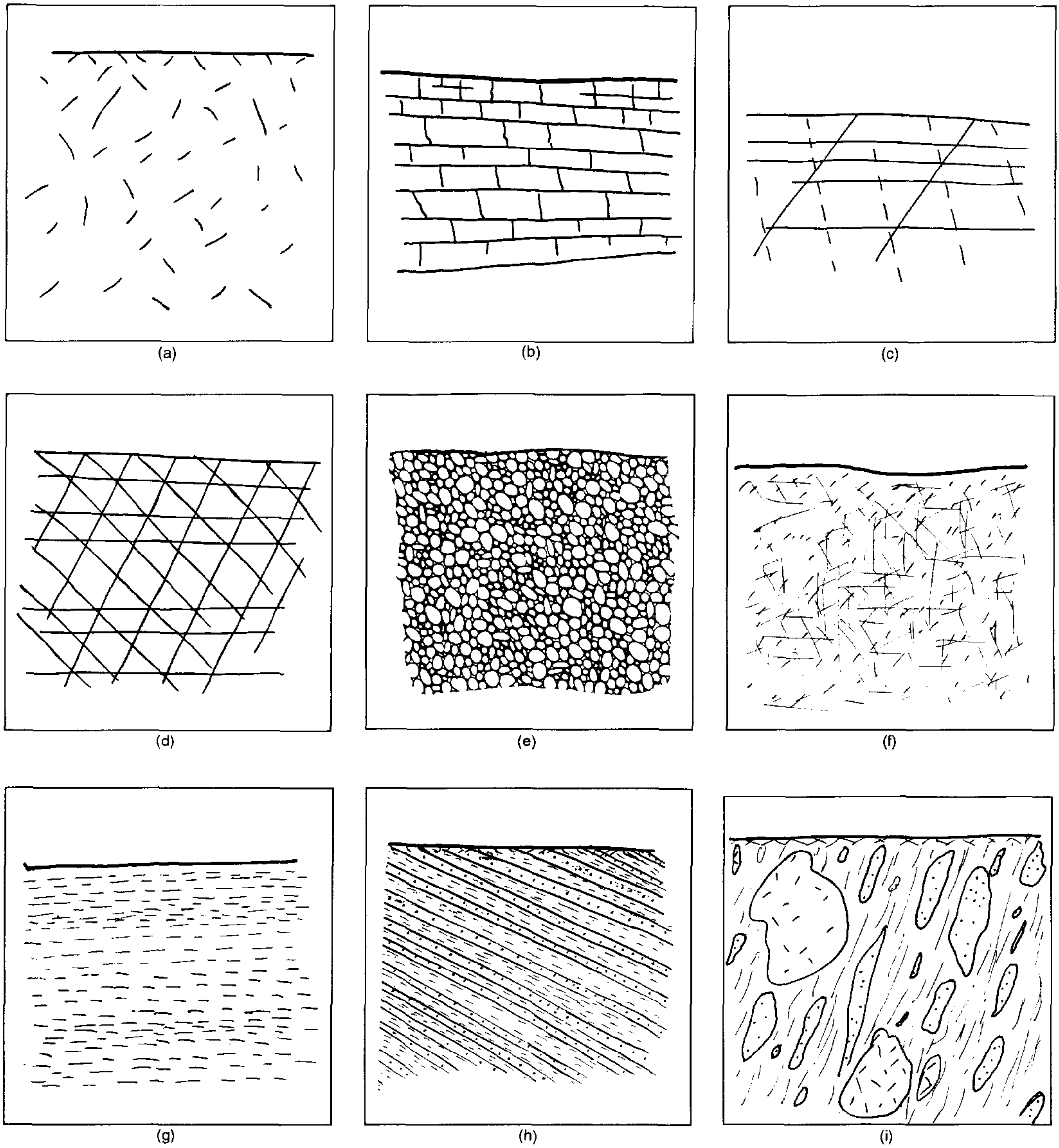

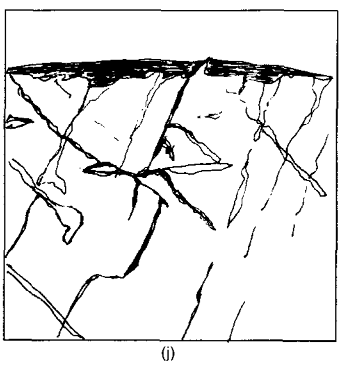

Fig. 1. Kinds of rock mass attributes: (a) jointless rock; (b) incompletely jointed rock; (c) incipiently blocky rock; (d) blocky rock; (e) highly porous rock; (f) highly fissured rock; (g) squeezing or swelling rock; (h) regular mixtures; (i) random mixtures; (j) cavernous rocks

surface. Blocky rock includes rock masses which are regularly cut by extensive joint sets in highly determined orientations, and rock masses which are variably and randomly cut by non-extensive joint sets in statistically dispersed sets of orientations, as well as all intermediate structural conditions. Block theory pertains primarily to rock in this class, for which methods of continuum mechanics are not well suited.

(*e*) In *highly porous rocks* (Fig. 1(e)) significant porosity affects mechanical behaviour due to poro-elasticity, fluid content and its movement in the pore skeleton, and pore crushing under distortion or contraction. Selected and refined methods of continuum mechanics apply in these rocks.

(*f*) *Highly fissured rocks* (Fig. 1(f)) have closely-spaced short fractures which engender high brittleness as well as great anisotropy, and significant non-linearity in virtually all mechanical properties. Sampling and testing are very difficult. These materials may resemble stiff-fissured soils in their mechanical behaviour.

(*g*) *Squeezing or swelling rocks* generally contain active clay minerals whose reactions with water impress immediate or delayed cracking, volumetric changes and distortions that may dominate rock mass behaviour (Fig. 1(g)). These rocks may soften appreciably on exposure to the agents of weathering. Soil mechanics methods may be applicable in such rocks.

(*h*) *Mixtures of dissimilar rocks* include regular mixtures achieved through intimate interlayering (e.g. rhythmically bedded sandstone and shale) (Fig. 1(h)), isotropic, random mixtures (e.g. saprolyte with corestones), and foliated random mixtures (e.g. serpentinite and melange (Fig. 1(i)). Particular methods are being developed to handle such materials using equivalent material models (Lindquist & Goodman, 1994; Medley & Goodman, 1994).

(*i*) *Cavernous rocks* are mainly soluble limestone, dolomite, gypsum and rock salt and clastic sedimentary rocks bonded by soluble cement (Fig. 1(j)).

More than one condition may pertain to a specific rock mass and even to a specific subdomain of an engineering site. For example, a highly porous rock may be blocky; a decomposed rock may be highly blocky owing to the formation of residual clay along discontinuities; or blocks of a rock mass may contain non-continuous fissures. For the application of block theory, the blockiness of the rock mass is concentrated on despite other important attributes. Thus even a decomposed granite, a porous diatomite or a folded interbedded sandstone–shale formation may satisfy the assumptions of block theory.

PROBLEMS OF CHARACTERIZING BLOCKY ROCK

For the simplest analysis using block theory, each joint set is represented by a single nominal orientation and a friction angle. Characterization of the joint system may be straightforward but it may also be complexly judgemental. The following are some sources of complexity.

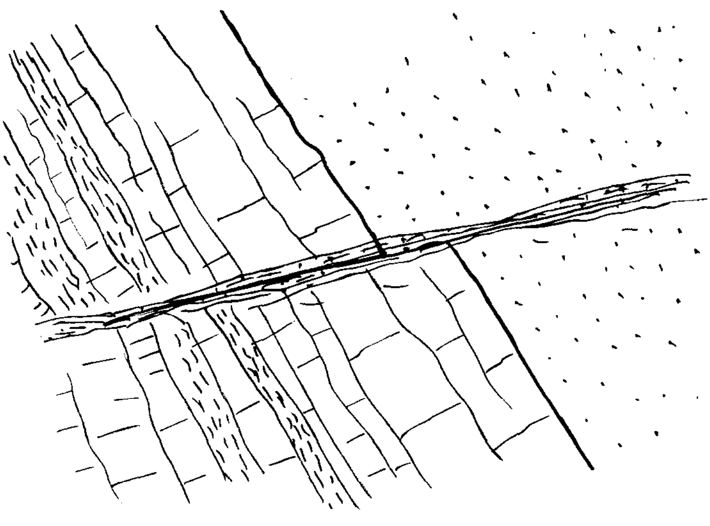

Fig. 2. Statistical joints and deterministic faults and contacts

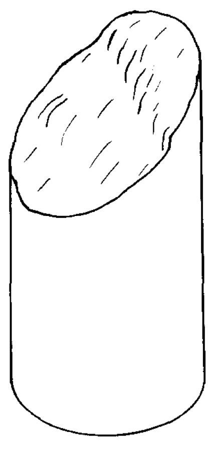

Fig. 3. Coarse roughness of a joint crossing a core sample

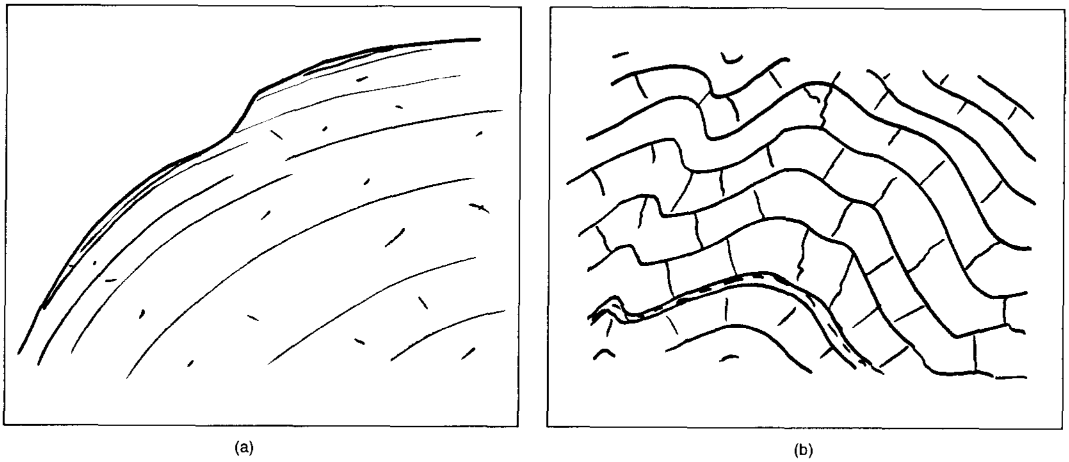

Fig. 4. Curved joints: (a) sheet joints; (b) folded bedding joints

Joint misidentification

In blocky rock, a joint is defined as an open discontinuity which lacks tensile strength or significant cohesion. In outcrops only portions of lines along the traces of joints can be seen and, although they may appear to be open, this condition may change a short distance into the outcrop. Fractures observed in drill core may have been reopened only during drilling.

Weathering

Mechanical weathering processes open joints that may previously have been tightly closed and develop incipient joints; chemical weathering processes accentuate the weaknesses and accessibility of joint surfaces. Thus in outcrops in the weathered zone, joints may seem more important than they really are. Conversely deposition of weathering products over the joint traces in the outcrop surface may mantle and obscure important individual discontinuities. Yet most geological observations at sites are conducted in the weathered zone.

Size effect

The volume of rock observed in the exploration of a site is usually much smaller than the volume which potentially supplies key-blocks to an engineering excavation. Most joints, like the crossing fractures in Fig. 2, are statistical data points in a large population and a minimum sample size is necessary to draw defensible generalizations. Adequate stochastic methods are being developed to characterize joint orientation, persistence and spacing. However, except for important individual joint surfaces like the mappable fault and formational contacts in Fig. 2, the actual location of any joint cannot normally be determined.

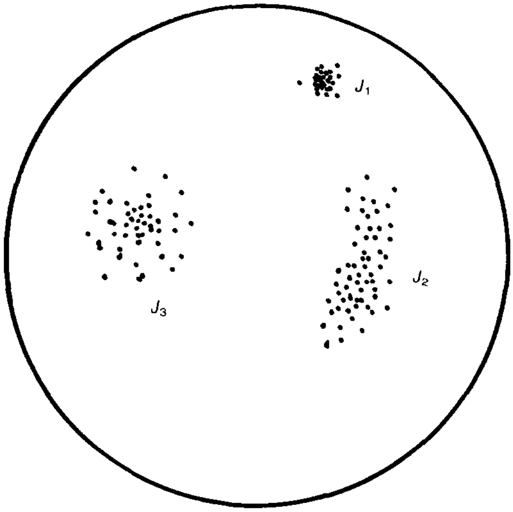

Fig. 5. Orientations of individual joints cluster in sets of varying degree of dispersion

Sampling difficulty

The shear strength of a joint depends to a great extent on the roughness of the joint, but the coarse scale of roughness of common discontinuities (Fig. 3) makes the required specimen size for acceptable shear tests large; accordingly, most joint samples acquired in exploration by drill holes are unsuitable for shear or triaxial compression tests.

Joint non-planarity

Block theory assumes that all joints are perfectly planar. Although this model is frequently satisfactory, errors could arise from misrepresentation of curved joints. Sheet joints (Fig. 4(a)), for example, and joints in severely folded rocks (Fig. 4(b)) are usually curved, as are some fractures at plutonic margins.

Dispersion in joint orientations

When one or more joint sets is highly dispersed, characterizing those sets by a single nominal orientation may be misleading. Statistical block theory can be applied only up to some degree of randomness. Consider the rock mass characterized by the family of joint orientations shown in Fig. 5, which is a stereographic projection of normals to individual joints; joint set J_1 can be well represented by a single measure of the distribution of normals, whereas set J_3 and the folded set J_2 are perhaps too widely dispersed to be represented by a single measure of the distribution of orientations. (The stereographic projection is discussed later in this lecture.)

GAINING DATA ABOUT JOINT SYSTEMS

Despite these complexities, geological mapping of natural and artificial exposures and the logging of boreholes usually provide good geometric data about the joint system. Tests on blocks in the field, back-calculations of natural block failures and, to a lesser extent, laboratory shear tests provide joint friction angles. These subjects are well covered in the geotechnical engineering literature (e.g. Hoek, 1983; Hoek & Bray, 1981; Barton & Choubey, 1977; ISRM Commission, 1978; Goodman, 1989) but some discussion is appropriate here. In general it is far easier to describe the orientations, spacings and frictional properties of joints than it is to attempt to quantify the hydraulic or mechanical properties of the rock mass itself.

Joint orientation and spacing are best determined by mapping traces along scan lines on outcrops or artificial excavations (Priest, 1993a, 1993b). The US Bureau of Reclamation prepares annotated overlaps for large colour prints which cover all exposed outcrops in and around a foundation or abutment; the attitudes of all joint traces are obtained by climbing to the trace or, if that is impractical, by using photogrammetry (Goodman & Scott, 1994). Where the soil cover is sparse, Barton & Larsen (1985) used hydraulic nozzles to wash soil from rock surfaces for the detailed mapping of exposed joint traces (Fig. 6). Fig. 7 shows a joint trace map prepared by the US Army Corps of Engineers who logged the

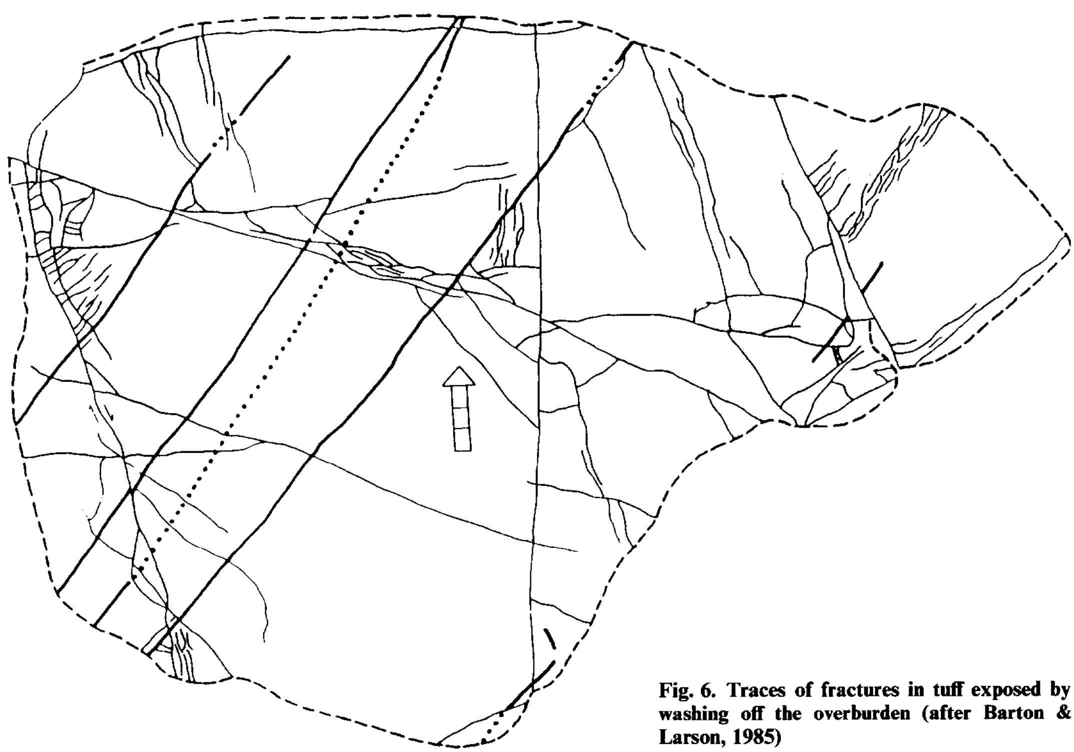

Fig. 6. Traces of fractures in tuff exposed by washing off the overburden (after Barton & Larson, 1985)

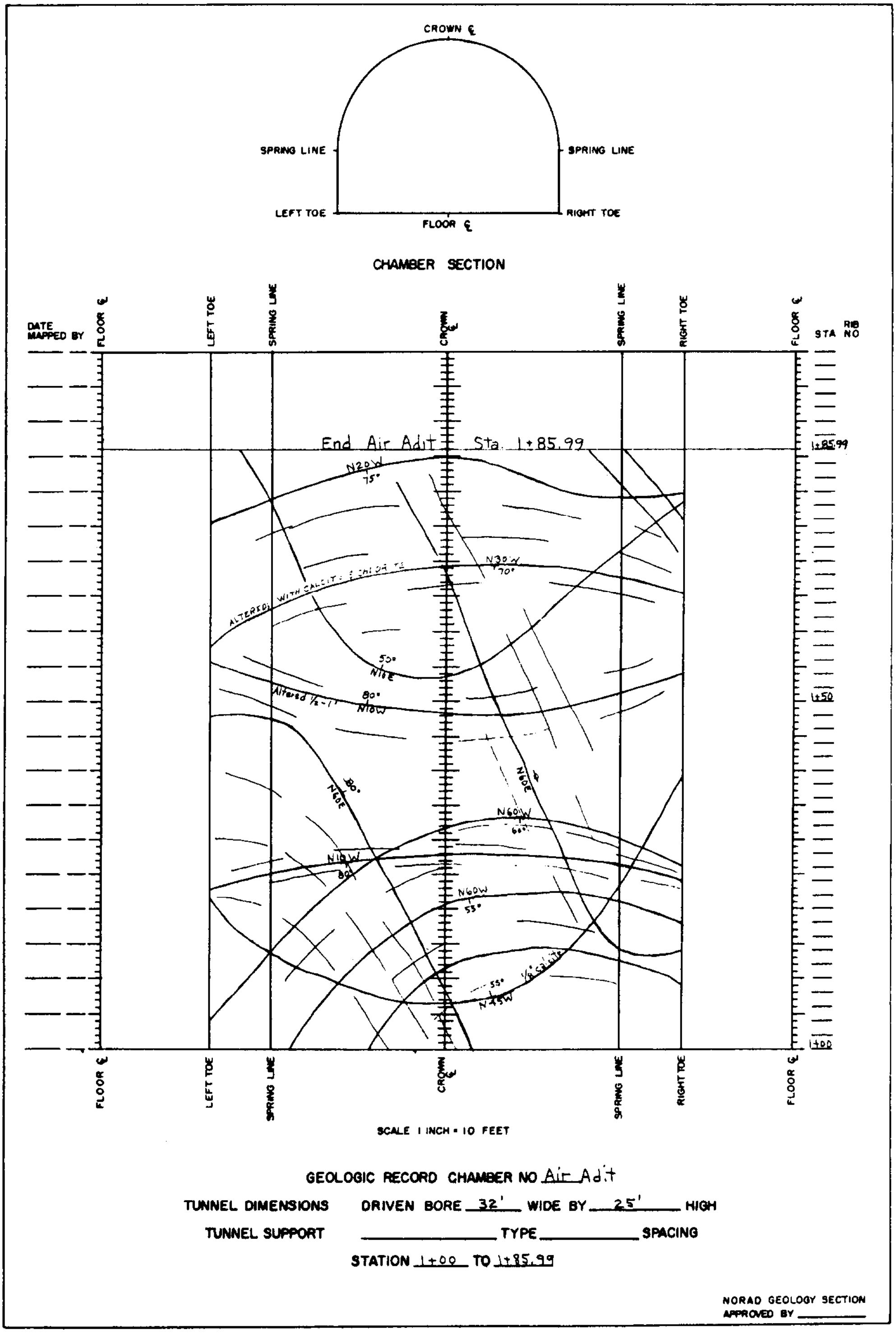

Fig. 7. Curved traces of planar joints produced by unrolling a map of the interior wall of a tunnel in the Norad complex, Colorado

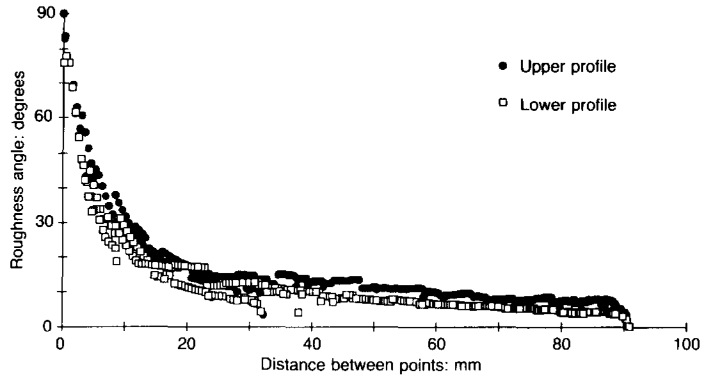

Fig. 8. Rengers' envelope of roughness angles produced by Thapa (1994) from data of the Core Corporation borehole scanner

walls of a cylindrical underground opening; curved traces result when the lines of intersection of the obliquely inclined joints on the tunnel walls are unrolled to produce a developed plan.* Such trace maps have been prepared as construction logs by many engineering organizations in the USA, Canada, Australia and elsewhere for at least 50 years,† but until recently I suspect that little direct use was made of them. With the development of block theory, trace maps become highly relevant and usable.

It is possible to determine joint orientation and spacing from drill holes by the acquisition of oriented core or the logging of the walls of the hole by a borehole scanner, a borehole televiewer, a borehole TV, a multi-arm caliper, an electrical resistivity dipmeter or downhole radar. Currently the best tool for logging fractures exposed in the walls of a hole is the borehole scanner, which acquires high resolution data at great speed and presents it in a format which can be processed (Tanimoto, 1988). In research at Berkeley, using the Core Corporation scanner, Thapa (1994) developed procedures to analyse the detailed expression of the trace of each joint to discern not only the absolute orientation of a joint (which is routine with this type of instrument), but also its aperture, roughness anisotropy and dilatancy. For example, Fig. 8 shows Rengers' (1970) envelope to roughness angles developed independently by Thapa for both the upper and the lower surfaces of a joint from a borehole scanner record. Fig. 9 shows a curve of dilatancy computed from the scanner data for a simulated direct shear test on the joint. From the latter, by assuming the basic friction angle for the joint, the joint shear strength and stiffness can be estimated. This area of technology can be expected to expand rapidly.

The friction angles of joints can be developed in a battery of field tests conducted on exposed outcrops. Many methods can be adapted for doing this. Frequently sections of the surface of steeply inclined joint surfaces are exposed in rock cuts where a former block has removed itself. For such joint surfaces, which invariably incline more steeply than the friction angle (Fig. 10), the friction angle can be calculated from the difference between the weight of a block hanging free and the force F_s required to sustain it in a state of limiting downslope sliding (or upslope sliding) against the rock surface.

Figure 11 shows another way to obtain the friction angle of an exposed joint surface inclined more steeply than the friction angle. The block is brought to a state of limiting equilibrium in an induced wedge mode by the introduction of a known, second sliding plane (e.g. a wooden block). The two blocks are then rotated about the normal to the unknown plane. The friction angle is calculated from the critical rake angle at which the block is in a limiting state, together with the

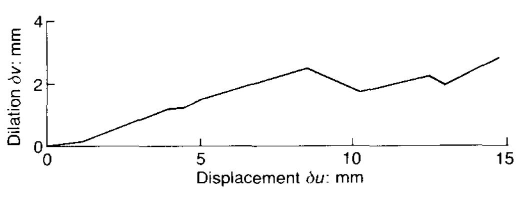

Fig. 9. Dilatancy curve computed from borehole scanner data by Thapa (1994)

* US Army Engineer District Omaha, Protective Structures Branch, Drawings made for a supplementary powerplant at Norad, and for the project Piledriver test.
† Examples of such logs may be found in the construction records of the Grand Teton Dam by the US Bureau of Reclamation, and of underground powerhouses T1 and T2 by the Snowy Mountain Hydroelectric Authority.

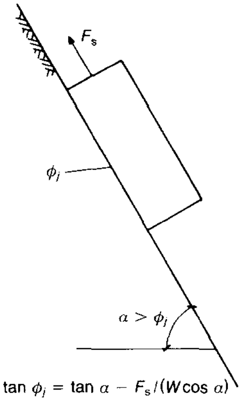

Fig. 10. Measurement of joint friction angle for the surface of a block held in a state of limiting downslope sliding

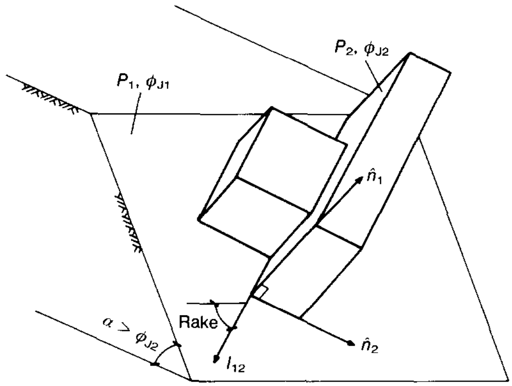

Fig. 11. Measurement of the joint friction angle for the surface of a block held in a state of limiting wedge sliding; the second surface of the wedge is introduced artificially

inclination of the unknown plane and the friction angle of the known second plane.

On artificial exposures of joint surfaces which dip more gently than the friction angle, blocks can be jacked into a limiting equilibrium state. Barton & Bandis (1983) have shown how to make effective use of various kinds of tilt tests for joints of low to moderate roughness. Moulds of blocks that have slipped out represent failure cases that can be back-analysed to yield the friction angle, subject to assumptions about water pressures or dynamic loads that may have existed at the time of failure.* Where the potential benefits of refining knowledge of the friction angle are sufficiently great, block samples can be drilled or mined out and tested in a laboratory.

ASSUMPTIONS FOR BLOCK THEORY AND REFINEMENTS

The underlying axiom of block theory is that the failure of an excavation begins at the boundary with the movement of a block into the excavated space. The loss of the first block (e.g. the shaded wedge in Fig. 12) augments the space, possibly offering an opportunity for the removal of additional blocks, with continuing degradation possibly leading to massive failure. The definition of a true key-block (Warburton 1987) would require degradation of a larger mass of blocks to result from its removal; presumably Warburton's numerical programs can perform this type of interaction analysis, as could three-dimensional discrete element or discontinuous deformation

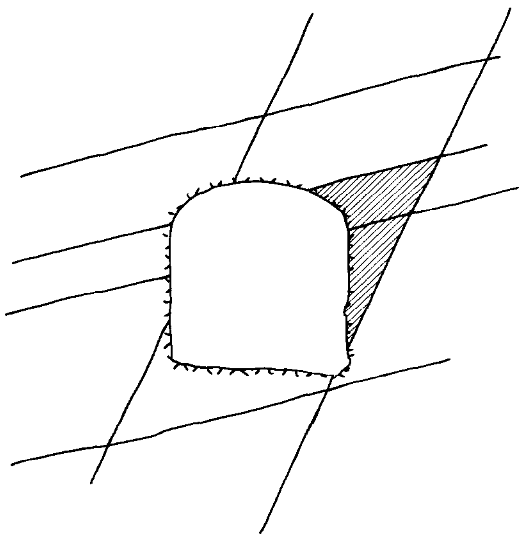

Fig. 12. Key-blocks (shaded areas) of an underground chamber

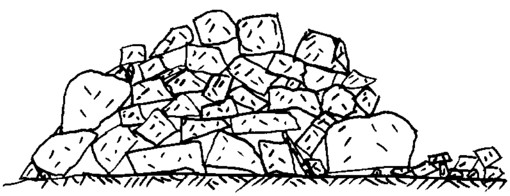

Fig. 13. Loosened block rubble for which the fundamental axiom of key-block theory could not be justified

* The term 'mould' in this usage was initiated by Hatzor (1992).

analysis if the correct joint attitudes were input. The term key-block as used here, however, identifies any block that would become unstable when intersected by an excavation. The identification of such a block therefore depends not only on the system of joints but also on the configuration of the excavation. The loss of a key-block does not assure a wider instability but the prevention of its loss does assure stability.

In a loose block system that has already undergone significant deformation (as in Fig. 13), a mode of failure through the retrogressive removal of blocks may not be applicable. In such rocks, massive failure may be preceded only by deformations within a multiblock group. In such an instance the underlying precept of block theory is violated and a more realistic model is required. However, any model such as key-block theory must respect the true three-dimensionality of the stability problem.

Blocks are generated by the intersection of pre-existing joints and surfaces of the excavation. It is assumed that a given joint plane is fixed in orientation but that its actual location can be varied continuously to establish the most critical position; this critical position is that which, in combination with other joints, determines a maximum key-block such that any larger similar block would no longer be removable. A maximum key-block is shown by the hat-shaped area above the underground chamber in Fig. 14.

The concept of a maximum key-block permits engineering design for jointed rock without specific knowledge of joint spacings, lengths or locations. When such information can be acquired, the maximum key-block can be replaced by a probable maximum key-block. McCullagh & Lang (1984), Kuszmaul (1992), Kuszmaul & Goodman (1992) and Mauldon (1992b) have discussed the probability distribution for key-blocks formed of infinite joints; Mauldon (1995) discusses the same for blocks formed with impersistent joints. The stochastic analyses of simulated joint networks can be used repeatedly to estimate size distributions for probable key-blocks (using the Poisson disk model (Baecher, Lanny & Einstein, 1977; Chan & Goodman; 1993)), or other two-dimensional or three-dimensional algorithms (Maerz & Germain, 1992).

In particular cases where the co-ordinates of points on actual locations of block-bounding joints can be obtained from boreholes or adits, the actual block sizes can be incorporated. If it can be afforded, there is merit in designing for the maximum key-block because such a design errs on the safe side.

Friction angle of joints diminish with increasing block weight, as shown in Fig. 15, so that the largest of a set of similar blocks will prove to be the least stable. Furthermore, the dimensions of the maximum key-block will establish the absolutely safe, minimum embedment depth for anchorage.

Although joints are assumed to be planar, the excavation shape can be complex. Many real problems can be solved with a single planar excavation surface; others require even non-convex spaces formed by intersecting excavation surfaces, or cylindrical surfaces generated by a family of lines parallel to a tunnel or shaft axis. As shown in Fig. 7, unrolling of the tunnel cylinder then produces curved traces that intersect to form

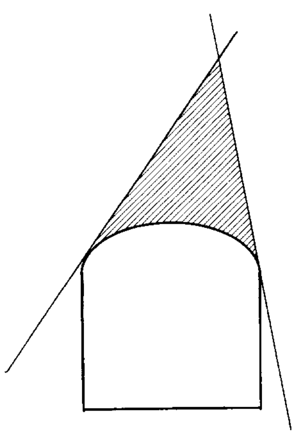

Fig. 14. Area of the maximum key-block A_{mkb} for an underground opening

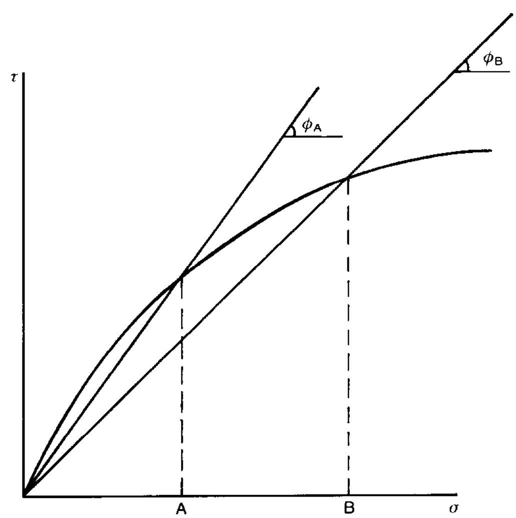

Fig. 15. Joint friction is smaller for a larger block

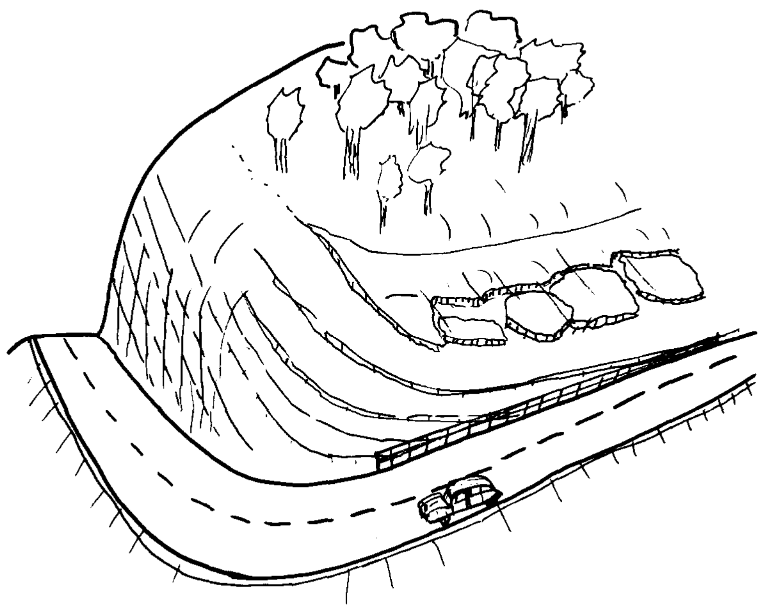

Fig. 16. Directionality of critical slope angle in a blocky rock mass

curved polygons, some of which are the faces of key-blocks (Shi & Goodman, 1989).

Key-block theory assumes the blocks to be rigid. Numerical modelling permits this restriction to be relaxed. In the case of a two-dimensional analysis of a toppling rock slope, a comparison between limit equilibrium analysis and numerical modelling by the DDA method showed that the minimum friction angle required for stability could be increased by prefailure deformations in the rock slope (Ke, Thapa & Goodman, 1994). Thus an assumption of rigidity may not always be conservative. The assumption that blocks are rigid need not affect the application of the kinematic, geometric portion of block theory even if it affects the determination of limiting equilibrium.

The deformability of the rock and the stiffness of the bounding joints affects the stability of a key-block subject to initial tractions across its faces. This problem has been discussed by many, including Crawford & Bray (1983), Karzulovic (1988), Yow & Goodman (1987), and Goodman, Shi & Boyle (1982). In the periphery of a rock slope or surface excavation, and in the destressed zone of an underground opening, the assumption of rigidity is not limiting. However, in some cases it may be inappropriate to ignore rock deformability.

In the original presentation of block theory, only sliding modes were considered. Wittke (1965, 1984) discussed the kinematics and analysis of rotational and sliding/rotational failures for prismatic blocks and wedges. Mauldon (1992a) subsequently extended block theory to embrace rotational modes of tetrahedral key-blocks with three joint sets.

FLOW OF IDEAS IN APPLICATIONS OF BLOCK THEORY

The most significant distinguishing attribute of blocky rock is perhaps its large directionality. For example, the rock mass in Fig. 16 is marginally stable at a relatively flat slope in the right of the drawing but is amply stable on a nearly vertical face with a different direction on the left of the drawing.

Joints are highly anisotropic with respect to mechanical and hydraulic properties; so are blocks which rest on joint faces, whose modes of behaviour are determined by the relative orientations of faces and edges and the relative positions of their corners. This great anisotropy makes problems of slope stability in blocky rocks different from those usual in soils. Suppose a rock mass contains a fault with soft clay filling and lack of easy drainage, such that its applicable shear strength is nearly zero. Even in this case, it may be possible to find directions for a safe vertical cutting through the rock mass. However, this advantage can be realized only by retaining the three-dimensional geometry of the design problem.

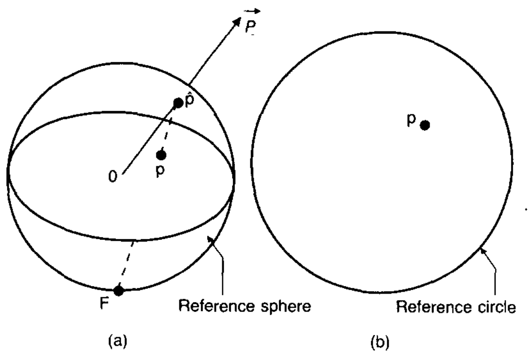

Fig. 17. Stereographic projection of an inclined line

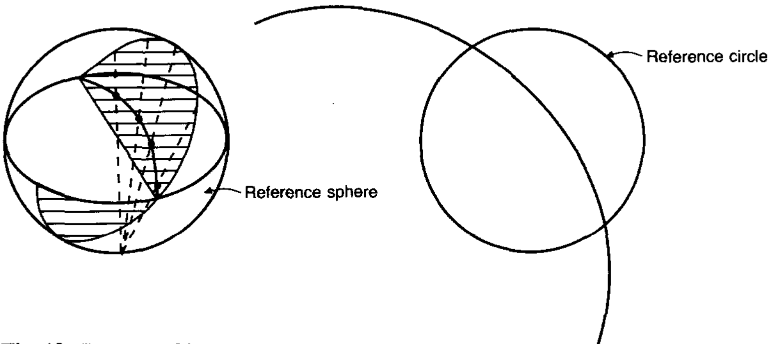

Fig. 18. Stereographic projection of an inclined plane

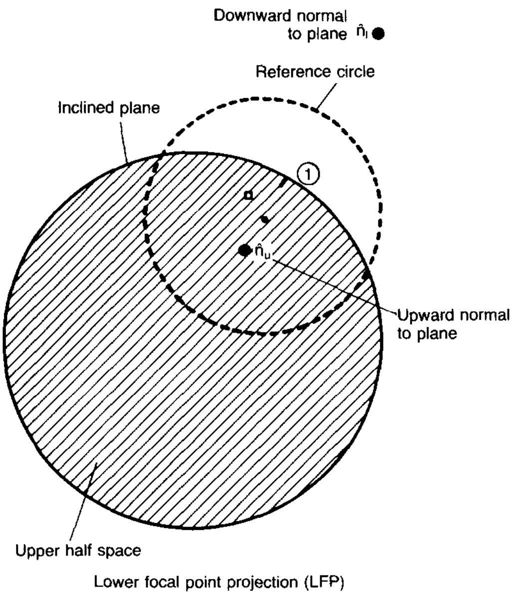

Fig. 19. The two half spaces of an inclined plane: if the focus of the projection is at the nadir point of the sphere, the shaded region inside the great circle is the upper half space

Table 1

Joint set	Dip angle	Azimuth of dip direction
1	50°	220°
2	40°	170°
3	20°	70°

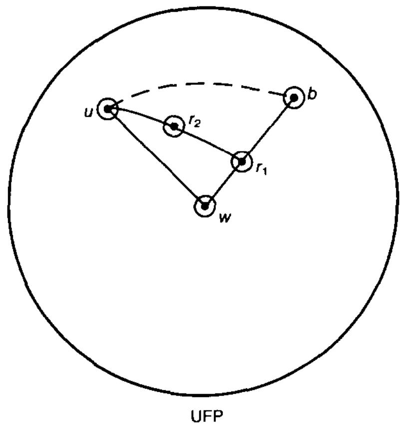

Fig. 20. Projection of the direction of a force resultant

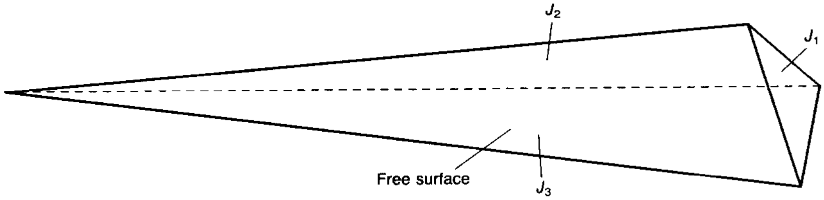

Fig. 21. Tetrahedral block with three joints and one free surface

Stereographic projection for block theory

The three-dimensional stability analysis can be handled by vector equations, whereas block theory gives birth to vector inequalities. Stereographic projection greatly facilitates the solution of both vector equations and inequalities by giving the analyst a physical understanding of the elements of any solution. In the case of simultaneous vector inequalities, the solution of which is not part of the training of most geotechnical engineers,* the stereographic projection offers a clean graphical solution.

Several uses are made of the stereographic projection here. The following points should be noted.

A point in the projection plane represents the direction of a vector whose tail is placed at the origin of a reference sphere. In Fig. 17(a) an upward vector P radiates from the centre of a reference sphere of arbitrary radius. The piercing point p of the vector on the sphere is projected to the diametral plane of the reference sphere by the line pF to a focus F at the nadir point of the sphere. The stereographic projection of the vector is represented by the intersection point p of the line pF with the diametral plane. Fig. 17(b) is a view looking down on the projection plane.

A plane (always assumed to pass through the centre of the reference sphere) projects as a great circle on the stereographic projection, as shown in Fig. 18. The two opposed normals to the plane are opposite points in the projection: one lies inside the plane's great circle and the other lies outside it (Fig. 19). Any such plane divides all directions into two subsets, which are the two hemispheres inside and outside the great circle. These hemispheres are termed the upper and lower half spaces of the plane.

A force cannot be represented by magnitude or point of application but its direction can be projected as a particular point. In Fig. 20 the force of given size in the direction w has a local resultant r_1 when it is added to a force of given magnitude in direction b. The addition of a third given force in the direction u then produces the resultant r_2 etc. In this way any system of forces passing through a single point can be represented by a particular point in the stereographic projection.*

Methods for plotting the stereographic projection of a given line, plane or cone, are presented in numerous references, including Goodman (1976, 1989), Goodman & Shi (1985), Heok & Bray (1981) and Priest (1985, 1993a). Although it is simple to construct a stereographic projection using only a compass and ruler, the more usual method involves tracing points and circles from a stereonet.

A stereonet presents a family of great circles representing planes that have a common intersection; these are analagous to lines of latitude on the globe. These great circles are cut by an orthogonal system of circles analagous to lines of latitude on the globe. The lines of latitude calibrate measurements of angles within the great circles.

Any line in space of known azimuth and plunge can be plotted as a point on a tracing over the stereonet as shown in all the cited references. As measurements of angles between two intersecting lines are always made in the plane common to these lines, it is convenient to measure such angles by marking on a tracing the points representing the lines, and then rotating the tracing on the stereonet to locate a great circle that intersects both; the required angle can then be found by counting the latitude lines between the two points. Projection of a plane from its known strike and dip is a matter of rotating the overlay and tracing a particular one of the great circles of the stereonet.

Most stereonets used for such geometric construction are prepared for one hemisphere of the reference sphere. For purposes of block theory, it is helpful to have a great proportion of the globe represented. Such a net† is shown in Appendix 1.

* Except perhaps for linear programming, which involves the solution of simultaneous, convex, vector inequalities by a simplex method.

* In Fig. 20, with downward force w, an upper focal point projection has been used to place the lower hemisphere inside the reference circle. In earlier figures, the lower focal point projection was used and the upper hemisphere occupied the region inside the reference circle.

† Computed by Gen Hau Shi and presented in Goodman (1989, p. 554).

The reference circle is no longer the outside boundary of the net, as in the hemispherical stereonet; otherwise, its use is similar. Given the strike and dip of joint planes, their great circles can be traced directly, as can be verified for the data presented in this lecture.

Joint pyramids and removability

A block with plane faces is the volume of intersection of four or more half-spaces. The tetrahedral block in Fig. 21 is an example; it is formed by the intersection of one free-surface half-space and three joint half-spaces. The orientations of the three joint surfaces are shown in Table 1.

All block-forming joint planes may be moved to pass through a single point (the origin); the volume of intersection of the block-side half spaces of the moved joints is called the joint pyramid (JP) of the block. Three joint planes produce eight such joint pyramids, as shown in Fig. 22. Each joint produces one great circle and the three intersecting great circles make the pretzel shape in Fig. 22. The spaces in the pretzel (i.e. the spherical triangles) correspond to the JPs. The digits identifying each JP are ordered according to the joint set number; 0 identifies the upper half space of a joint and 1 identifies the lower half space.

Similarly all the block-forming excavation planes (free surfaces) can be moved to pass through the same origin. The volume of intersection of these moved free surfaces is called the excavation pyramid (EP) of the block and its complement is the space pyramid (SP). The tetrahedral block in Fig. 21 had only one free surface, so its SP is limited by one circle. This is shown in Fig. 23, for a free surface dipping 48° to azimuth 35°.

Each joint system creates a particular pattern of JPs. For a particular set of joints, the individual JPs are an effective geometric and mechanical compartmentalization of the infinity of possible blocks, each JP producing its own sub-infinity of potential blocks.

If a JP plots on the stereographic projection, it can form blocks that can be moved physically towards the space; such blocks are called removable blocks. According to Shi's theorem (Goodman & Shi, 1985) a block is removable in a particular excavation if, and only if, its JP plots entirely within the SP of the excavation. The joint planes and the free surface are plotted together in Fig. 24, from which it can be seen that the only JP satisfying Shi's theorem is 110. Thus all blocks that are removable in the given excavation (i.e. in a rock slope dipping according to the orientation of the given free surface) must be formed by the volume of intersection of the lower half spaces of joint planes 1 and 2 and the upper half space of joint plane 3. This information is sufficient to locate the faces of such blocks on a map of the joint traces on the free surface.

Three joints are the minimum required to produce removable blocks in a planar excavation; in such an excavation a system of three joint sets will produce only one removable JP. A cylindrical tunnel produces six removable JPs for the

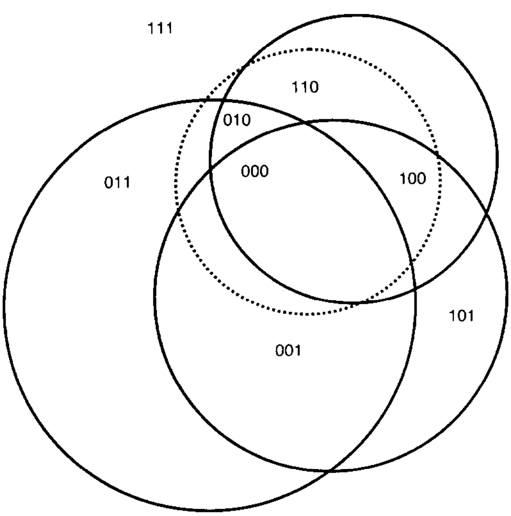

Fig. 22. Lower focal point (LFP) stereographic projection of three joint sets, giving eight JPs

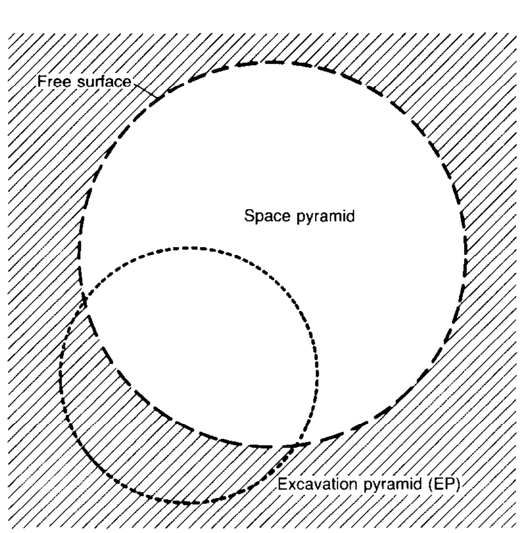

Fig. 23. LFP stereographic projection of the excavation pyramid (shaded) and space pyramid (unshaded) of a planar excavation (e.g. a rock slope)

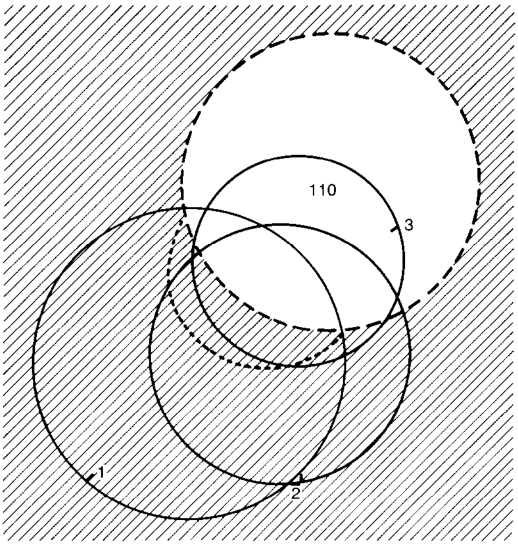

Fig. 24. LFP stereographic projection of the JPs and the space pyramid, which establishes by Shi's theorem that only JP 110 is removable

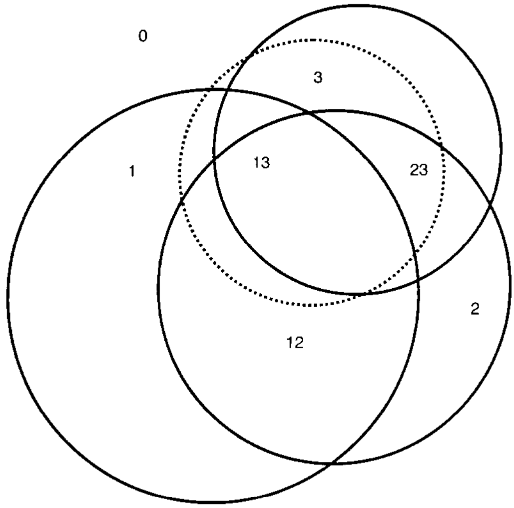

Fig. 26. Results of mode analysis giving the potential sliding mode for each JP under an assumed direction of the resultant force on any block, which in this example was taken as that of gravity

same three joint sets, but each is limited to a particular portion of the periphery, whose limits are easily determined from the application of Shi's theorem.

Translational modes of a removable block

Londe, Vigier & Vormeringer (1969, 1970) described the seven translational modes of a tetrahedral block with one free face and three joint faces. There are three modes of sliding entirely on one face, three of sliding on two faces simultaneously (along their line of intersection) and one of opening (lifting) from all faces. Fig. 25 depicts one of the three modes of sliding simultaneously on two faces.* Block theory presents two types of mode analysis to identify the appropriate sliding modes for a given joint system.

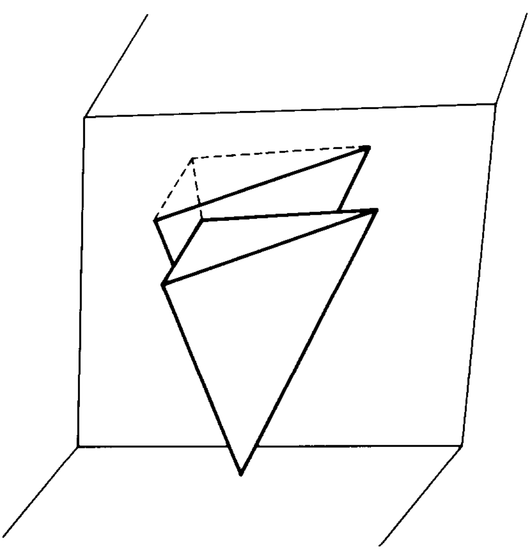

Fig. 25. Block translation by sliding along an edge

The first type of mode analysis identifies the appropriate mode for each JP of a joint system corresponding to a given direction for the resultant force acting on a block. Fig. 26 illustrates the mode analysis for the adopted joint sets under the resultant force direction corresponding to that of gravity. Once a resultant force direction has been selected, the locations of its projections on each of the joint planes establishes the mode corresponding to each JP. In Fig. 26, 1 means sliding on face 1, 12 means sliding on faces 1 and 2 simultaneously, and so on; 0 identifies the lifting mode. Each JP is identified by one and only one of these labels. If one particular joint is known to be weaker or more perilous than the others, an excavation direction can be sought that would cause the single removable JP to lack a mode of sliding on that joint.

The second type of translational mode analysis identifies the regions in which the resultant force

* Block theory has generalized Londe *et al.*'s solutions for an arbitrary number of joint faces, but the tetrahedral block is sufficient for this discussion.

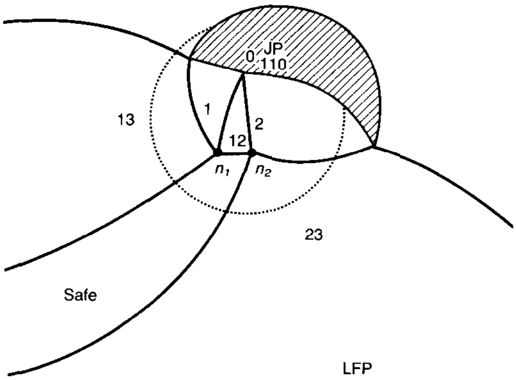

Fig. 27. Equilibrium analysis for JP 110, showing the different translational mode regions for this JP as the resultant force assumes different directions (lower focal point projection)

direction must plot corresponding to each sliding mode for a given JP. As shown by Londe *et al.* (1969, 1970), the mode regions of a given JP, in which the resultant force must plot, are contiguous polygons. Their united region embraces the entire reference sphere except for the polygon whose corners are the non-blockside normals to the joints of the JP; any direction in that polygon is safe, regardless of the magnitude of the friction angles on the faces. As contributors to the resultant force are added (e.g. by water pressures on the joint faces, inertia or rock reinforcement) the changing position of the resultant can be tracked and the corresponding changes in modes identified. Thus one can see immediately which types

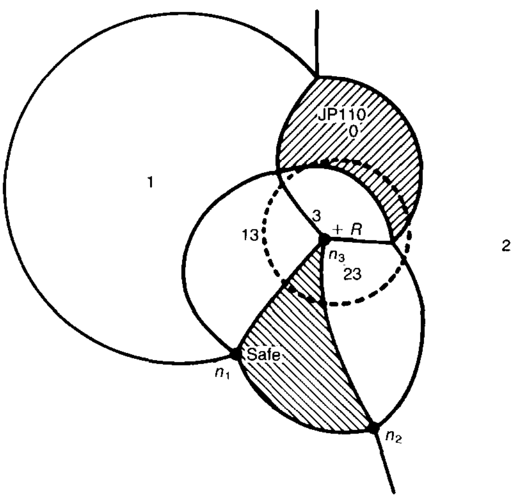

Fig. 28. The same information as in Fig. 27 but plotted with an upper focal point projection

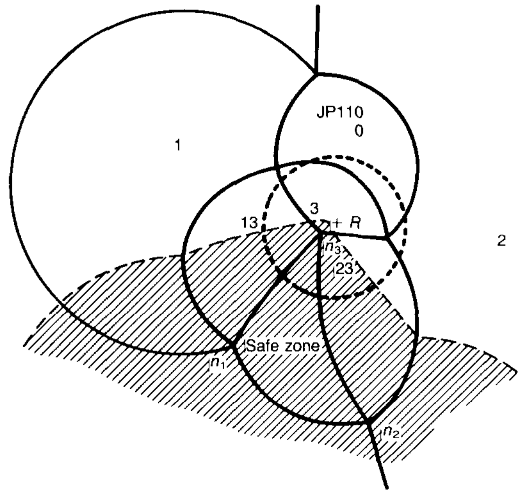

Fig. 29. Results of the equilibrium analysis for JP 110, with an upper focal point projection, and specific friction angles on each joint set (30°, 25° and 20° for joint sets 1, 2 and 3 respectively); when the resultant force has any of the directions in the shaded region, all blocks that have JP 110 will be safe against sliding

and directions of remediation measures will tend to be most effective.

Figure 27 is a projection of the selected JP 110 and the three normals pointing outwards from each block face (the non-blockside normals). Because one normal is pitched steeply downwards, its projection is far from the reference circle and cannot be shown in the figure. The great circles have been defined by all combinations of JP edges with normals, as shown. The resulting spherical triangles each bear a mode name, as discussed by Londe *et al.* (1969, 1970).

Stability analysis for a given JP

An equilibrium analysis for a block is relevant only if its JP is found to be removable in a particular excavation. Then, corresponding to given friction angles on the joints of that selected JP, the sliding mode regions can be divided into safe and unsafe parts.

The equilibrium analysis usually centres about the direction of gravity, and so it is more convenient to adopt an upper focal point for the stereographic projection, which places the gravity direction at the centre of the reference circle. Replotting the data of Fig. 27 with an upper focal point projection yields Fig. 28.

If the friction angles of all joint faces were equal to zero,* the JP would still be safe from

* Cohesion is assumed to be zero and so the shear strength is nil in this case.

sliding if the resultant force plotted in the polygon whose corners are the non-blockside normals to the joint planes. In Fig. 28, this region is the spherical triangle denoted as safe. The bounds of that polygon would now divide the whole sphere of directions into a set that is safe, and a much larger set that is unsafe.

If, at the other possible extreme, the friction angle on each joint plane of the JP were equal to 90°, the bounds of the safe region would be extended to the sides of the JP itself and all the directions of the resultant force would be safe except those which plot inside the JP itself. If the resultant force is directed in any of the directions of the JP, its blocks will tend to lift simultaneously from all joint planes (mode 0).

When the friction angles have real values between these extremes, the border of the safe zone loops around the JP as shown in Fig. 29. To construct this figure, the following friction angle values were adopted: 30° on joint plane 1, 25° on joint plane 2 and 20° on joint plane 3. The loop separating the safe from the unsafe directions is a small circle (the projection of the friction cone) in each mode region for sliding on a single face; it is a great circle in each mode region for sliding on two faces. The construction of the bounds of the safe zone and a method for reporting the factor of safety for sliding are discussed in many places (e.g. Goodman, 1976; John, 1968).

An important innovation introduced by Shi (Shi & Goodman, 1989) is the construction of a series of such loops for friction angles from 0° to 90°; the resulting field of friction contours shows the friction angle required for equilibrium (the mobilized friction angle) corresponding to any orientation of the resultant force and equal friction angles on each face. For example, Fig. 30, constructed according to this scheme, shows that the resultant force direction R identified by a cross, requires friction angles of at least 20° on each face to achieve equilibrium, i.e. when the resultant force is in the direction of R the mobilized friction angle is 20°.

Key-blocks

The sequence of analysis which is described determines

(*a*) if a joint half space combination (a JP) produces blocks that are removable
(*b*) the mode of sliding, if any, that is possible for such blocks under an assumed direction of resultant force (frequently that of gravity)
(c) whether or not any block of that JP is unstable without support.

A key-block is a block that is removable; it also has a sliding mode and it is unstable without support.

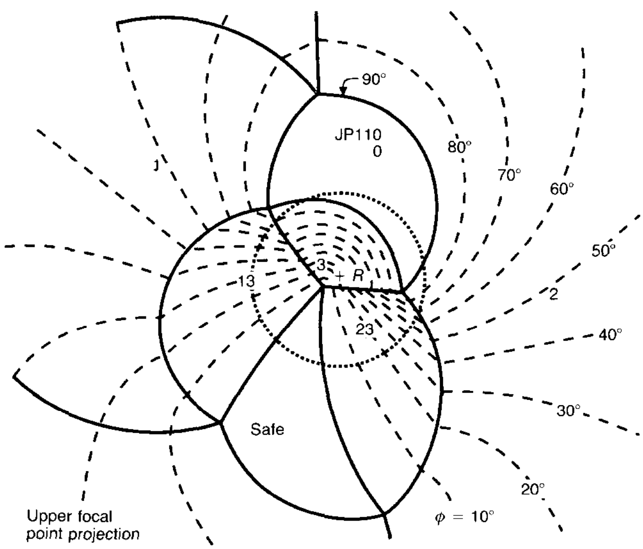

Fig. 30. Results of the equilibrium analysis for JP 110 as in Fig. 29; the boundary of the safe zone corresponding to equal friction angles on all joints is given by the appropriate contour (dashed line)

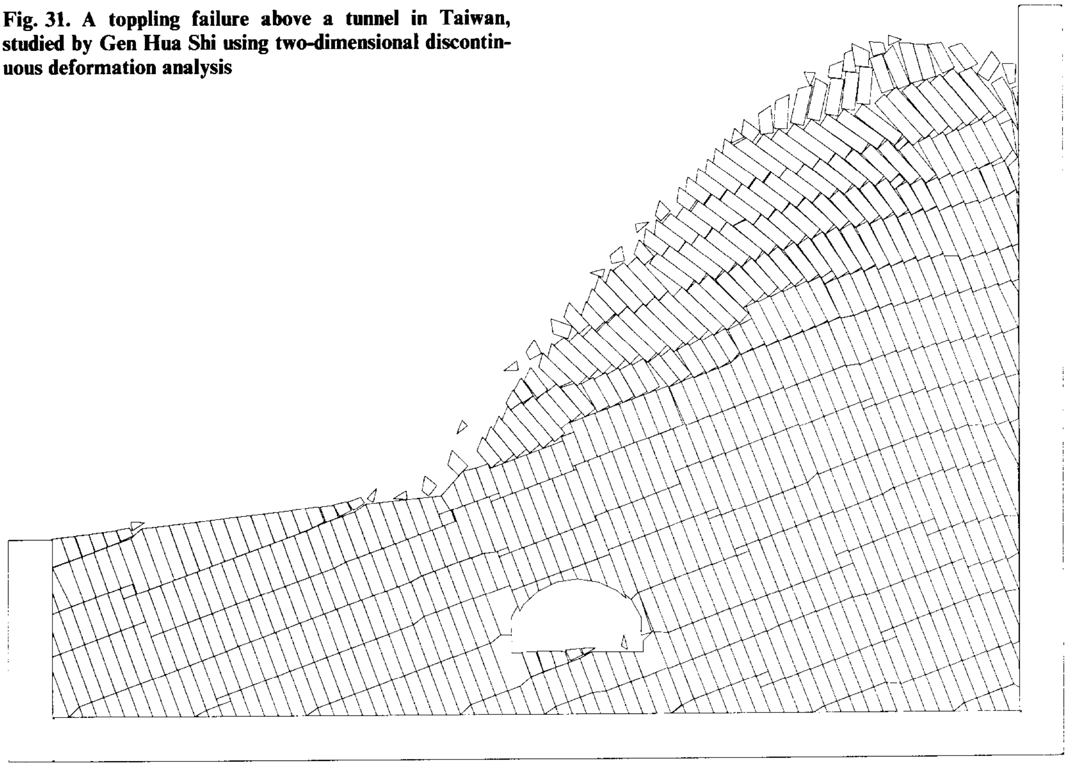

Fig. 31. A toppling failure above a tunnel in Taiwan, studied by Gen Hua Shi using two-dimensional discontinuous deformation analysis

BLOCK THEORY APPLIED TO ANALYSIS OF ROTATIONAL MODES

Block theory has been generalized to examine rotational failures of blocks by Mauldon (1992a) and Mauldon & Goodman (1990, 1995). Like the analysis of block sliding, rotational block theory considers first removability, then rotational modes, and finally rotational stability. This work extends to three dimensions the pioneering analysis of Wittke (1965, 1984) who identified a number of possible rotational movements for rock blocks.

A block can rotate in many ways. Best known is the forward rotation or toppling of a prismatic or tabular block about an edge in the free face (de Freitas & Watters, 1973; Goodman & Bray, 1977). Toppling failures of rock slopes occur widely in steeply dipping layered or foliated rocks in which the joints dip into the mountainside. Although this mode of failure was not well appreciated by many geotechnical engineers until relatively recently, its impact on engineering is substantial. Fig. 31 shows a discontinuous deformation analysis* of a large toppling failure that affected a tunnel in Taiwan.

* Conducted by Gen Hua Shi.

The analysis of toppling failure is complex because the number of degrees of freedom is large. However, from the point of view of block theory kinematics, it is a simple two-dimensional case. Slightly more complicated is the forward toppling of a tetrahedral block about an edge in the free face, as shown in Fig. 32. The edge about which the block rotates is the line of intersection of a joint plane of the JP and the free face. A block with one free face and three joint planes has three such edges and therefore offers, potentially, three such modes.

A tetrahedral block can also rotate forwards about an axis through a corner in the free face, as shown in Fig. 33. There are three such free corners where the lines of intersection intersect the free surface; each of these has, potentially, an infinity of potential axis directions.

Corner and edge rotation are examples of pure rotational modes, on which the reaction forces act only along the axis of rotation. At least two additional modes involve rotational sliding in which the joints rotate while maintaining some contact along an additional block edge or face: torsional sliding and block slumping.

In torsional sliding (Fig. 34) the block rotates about an axis normal to a joint face through a

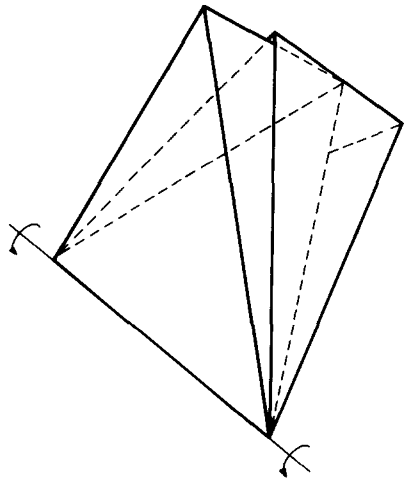

Fig. 32. Rotation of a tetrahedral block about one of its edges in the free surface

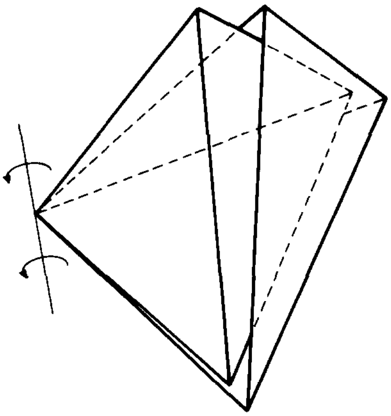

Fig. 33. Rotation of a tetrahedral block about an axis passing through one of its free corners, where an edge of the JP intersects the free surface

free corner, producing a torsional sliding motion along the joint. Block torsion was shown as the probable failure mode for the abutment of Malpasset Dam in a three-dimensional finite element analysis by Poisel, Steger & Unterberger (1991).

In block slumping (Fig. 35) the block rotates backwards as it slides along an edge-to-face or corner-to-edge contact. As discussed by Wittke (1965, 1984) the centre of rotation for a slumping prismatic block is known and a stability analysis can be made, the degree of safety being subject to an assumption about one reaction. However, little is known about the magnitude of limiting friction when an edge slides along a face, and

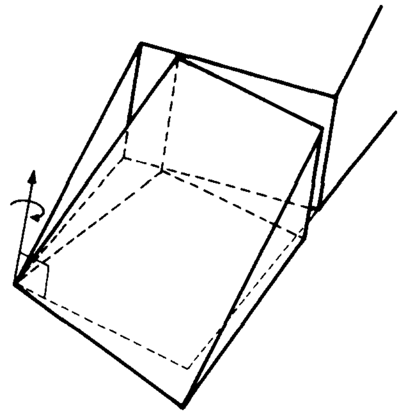

Fig. 34. Torsional sliding of a block

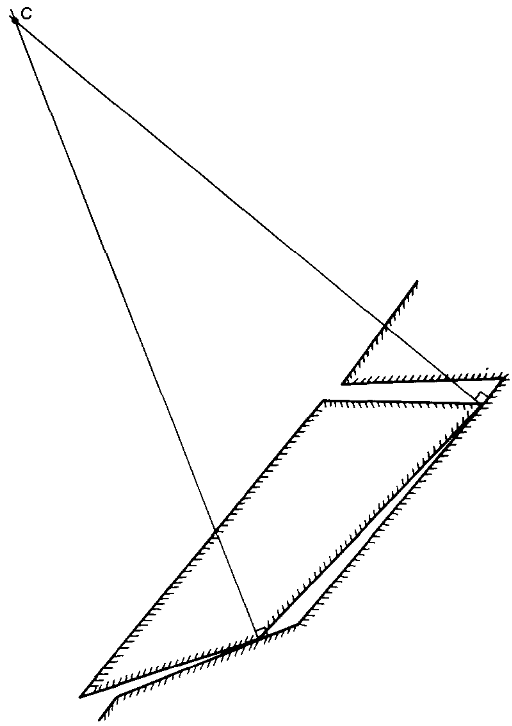

Fig. 35. Block slumping, with back turning rotation about point C

little is known about frictional properties in full-face torsional sliding along joints.

Removability in relation to rotational modes

Blocks with JPs having 1, 2 or 3 joints must be removable in order to have a rotational mode. Therefore rotational modes into a particular excavation can be ruled out for JPs (of three joints or less) that are not removable in that excavation. This is not strictly true with higher order JPs, as shown by Mauldon (1992a).

Rotatability of a JP

Consider rotation of a tetrahedral block formed from a three-joint JP about an axis through a free corner on the line of intersection of joint planes 1 and 2. The block is assumed to be rigid so there can be no interpenetration of the corner into the rock face. This means that the corner rotation must move all points along I_{12} into the half space of the blockside normals to planes 1 and 2. Pursuing this mathematically leads to the following condition of kinematic necessity for rotation about an axis through any point on I_{12}: at least one of the two sides of the JP spherical triangle extending from corner I_{12} must be greater than 90° (Fig. 36).

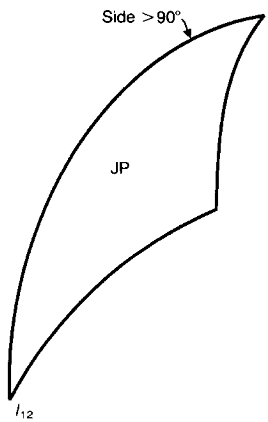

Fig. 36. Geometric condition required for rotation about an axis through corner I_{12}

Now consider rotation of the same tetrahedral block about an edge in any free face, e.g. an axis of rotation along the line of intersection of joint plane 1 with the excavation surface. On rotation, the movement of points on the free face will be in the direction of the blockside normal to joint plane 1 and this specific direction must be contained in the JP. Pursuing this mathematically leads to the following condition of kinematic necessity for rotation about any edge in face 1: both interior angles involving side 1 of the JP spherical triangle must be greater than 90° (Fig. 37). In this case, the blockside normal to face 1 must plot within the JP.

Edge rotation can be considered a special case of corner rotation in which the axis of rotation lies in one joint plane and extends from one corner to another. Therefore edge rotation cannot occur if corner rotation is kinematically inadmissible. It can therefore be concluded that a three-joint JP is non-rotatable if all its sides are acute, as in Fig. 38.

Some observations about the stereographic projection facilitate application of these rules. With three joint sets, the length of JP side 1, for example, corresponds to the angle between the traces of joint planes 2 and 3 in plane 1 and is easily measurable from the stereographic projection. The interior angles at corner I_{12}, for example, of a JP correspond to the dihedral angle

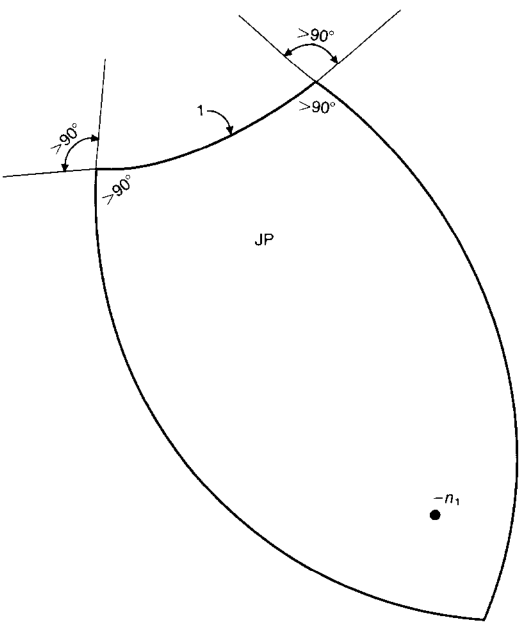

Fig. 37. Geometric condition required for rotation about an axis along a free edge in plane 1

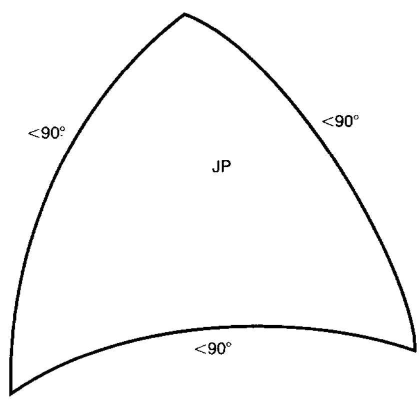

Fig. 38. A non-rotatable JP

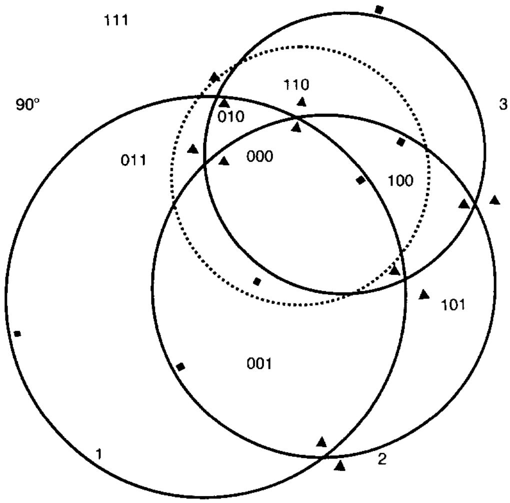

Fig. 39. Data to apply Figs 37 and 38 to all JPs is quickly obtained from the stereographic projection

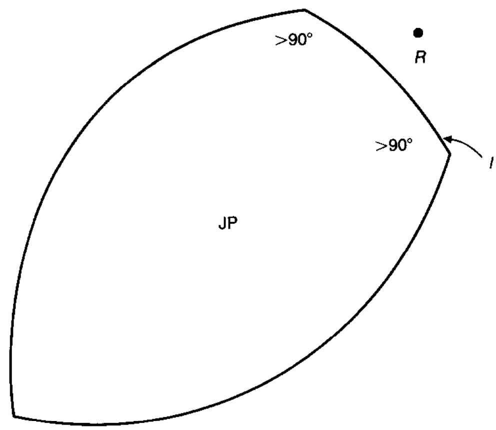

Fig. 40. R tends to cause rotation about an axis in face 1

between planes 1 and 2 and may be read with a protractor between the tangents to the sides at I_{12}. Given a stereographic projection of three joint sets, all the lengths and angles follow if they are measured for only one JP. Each JP can then be characterized according to the edges and corners about which it can be rotated. An example is given in Fig. 39.

Rotational mode analysis

The two types of mode analysis discussed for sliding can be made for rotations. If a block rotates purely about an edge in a joint face, the reaction force must intersect that edge and consequently the resultant force on the block must have a component directed into the non-blockside normal. Consequently, the resultant force vector must plot outside the JP, as shown in Fig. 40. Corner rotation is more complex; unlike the case of sliding, the corner rotation modes overlap part of the edge rotation modes.

Rotational mode analysis type 1 identifies the modes for each JP when the resultant force is fixed in direction. In a three-joint system, the two JPs that contain the direction of the resultant force or its opposite both lack a mode. Each of the remaining six JPs has a possible edge rotation or corner rotation mode which can be named according to the position of the resultant force on the stereographic projection.

The second type of rotational mode analysis identifies the modes for a given JP corresponding

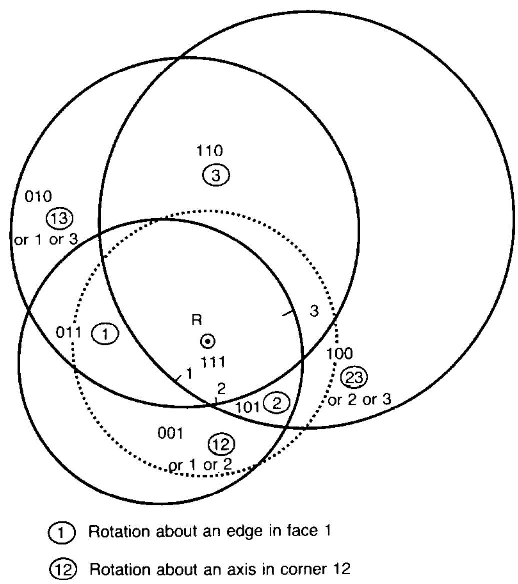

Fig. 41. Analysis of rotational modes for each JP given the direction of the resultant force

to different orientations of the resultant force (Fig. 41). Each corner of the JP has a contiguous corner rotation mode zone outside the JP in the region between the extensions of the two great circles that form the corner. Each JP side has a contiguous edge rotation region outside the JP. Unlike the mode analysis for sliding, the mode zones overlap. A specific free face limits the extent of both regions because the resultant force must plot in the space pyramid. For a planar excavation face, this means that the mode zones are restricted to lie in the half space on the non-blockside of the free face.

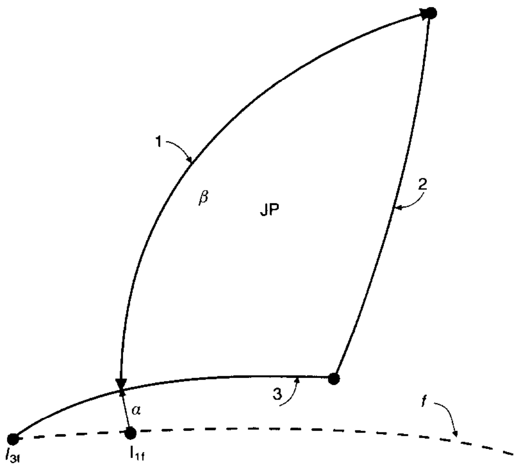

Fig. 42. Determination of the angles α and β

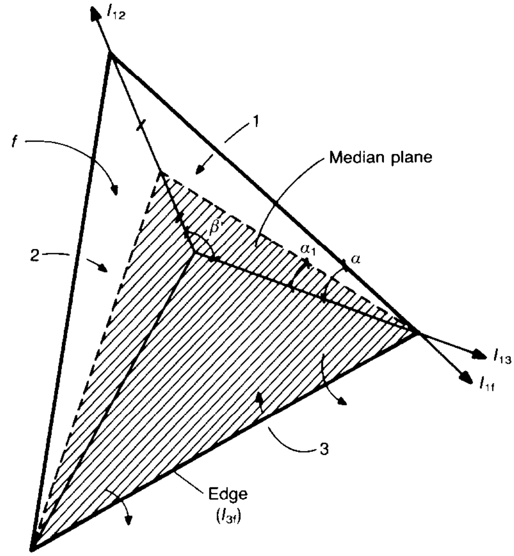

Fig. 43. Mauldon's median plane corresponding to a free edge and the angles α, β and α_1

Stability analysis for rotations subjected only to body forces

Rotational stability analysis can be simplified for the case of a tetrahedral block with three joint faces and subjected exclusively to body forces. Unlike the analysis of sliding stability, it is necessary to associate a particular free face with the JP to be analysed. With the free face added to the stereographic projection of the JP, the two angles α and β in Fig. 42 can be read from the stereographic projection. Then the stereographic projection of a median plane to the tetrahedron, as shown in Fig. 43, can be constructed from the calculated angle α given by equation (1)

$$\tan \alpha_1 = \frac{\tan \alpha \tan \beta}{\tan \alpha + 2 \tan \beta} \quad (1)$$

The method of developing the stereographic projection of the median plane for an example is shown in Figs 44 and 45. In Fig. 44 the two required angles are determined as shown. Entering these values in equation (1) allows construction of the median plane, as shown in Fig. 45. The constructed median plane now divides the edge

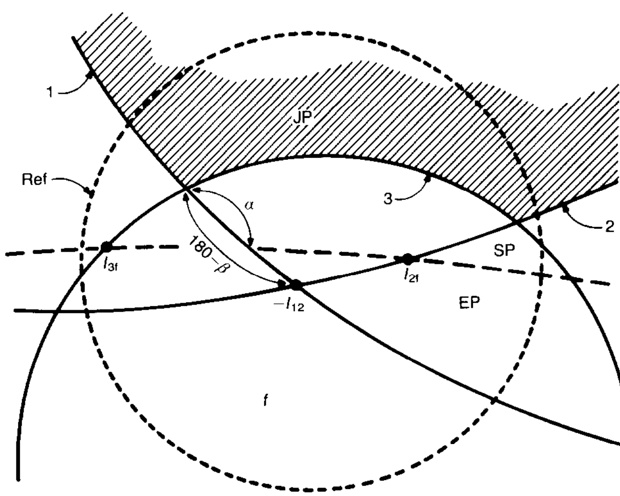

Fig. 44. Measurement of the angles α and β for an edge formed by the intersection of the free surface with plane 3

rotation region into unsafe and safe subregions. If the resultant force vector defines a point on the median plane, the block is in a condition of limiting equilibrium in rotation. Any orientation for the resultant force on the JP side of the median plane is unsafe.

Mauldon (1992a) offers an expression for the factor of safety with respect to edge rotation, making use of equation (1). He also shows how the line of intersection of the two median planes for the joint faces intersecting at a corner can be used to delimit mode regions for pure corner rotation and torsional sliding.

Rotational key-blocks

The sequence of analysis described determines

(*a*) if a joint half space combination (a JP) produces blocks that are removable
(*b*) the mode of rotation, if any, that is possible for such blocks under an assumed direction of resultant force (frequently that of gravity)
(*c*) whether or not any block of that JP is likely to rotate if it is left unsupported.

Negative results are valuable in that a block that fails any of these tests is not likely to be dangerous unless the assumptions prove unreasonable.

Stability analysis in more general cases

Given any direction of the resultant force on a block, and any known position and orientation of the axis of rotation, the overturning moment can be calculated by the classical vector equation for the moment of a given force vector acting through a known point about an axis in a given direction through another known point. As indicated by Wittke (1965) a block is to be judged unstable if there exists any net moment promoting overturning in an unsafe direction. Thus the stability can be assessed when there are non-body force components (see, for example, Goodman, 1976, pp. 231–237).

For rotation about an edge, the orientation of the axis of rotation is known and its location is generally determinable. Thus the moment equation can be applied if the resultant force vector is known in orientation and line of action.

For rotation about an axis through a corner, the position of the axis is generally known, but there are an infinite number of possible orientations for the rotational axis. Thus the moment equation cannot be used without further information. However, in this case it is possible to restrict the range of allowable orientations of the rotational axis using a set of inequalities expressing kinematic requirements derived by Mauldon (1992a) (Fig. 46). These formulate the kinematic requirement that all points along the three edges radiating from the axial corner must move, by virtue of the rotation, into the blockside half spaces of particular joints. This leads to the seven inequalities stated in Fig. 46, each one of which determines a half space that satisfies the inequality. The set of seven intersecting half spaces establishes a solution space in which the axis is constrained to lie.

Figure 47, from Mauldon (1992a) shows the solution space for a specific example. For rotation

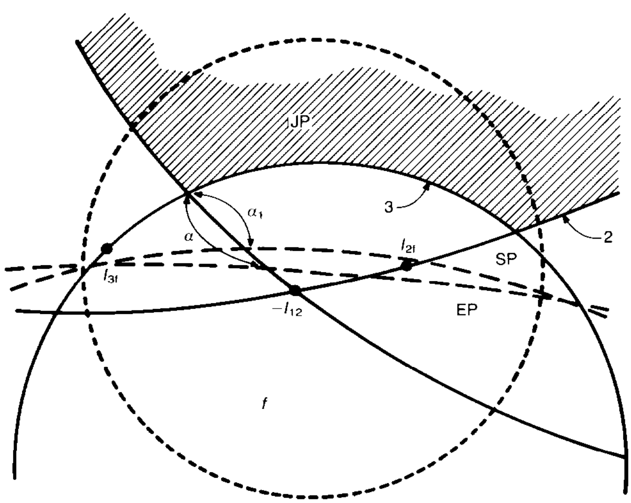

Fig. 45. Rotational equilibrium analysis under body forces by constructing Mauldon's median plane

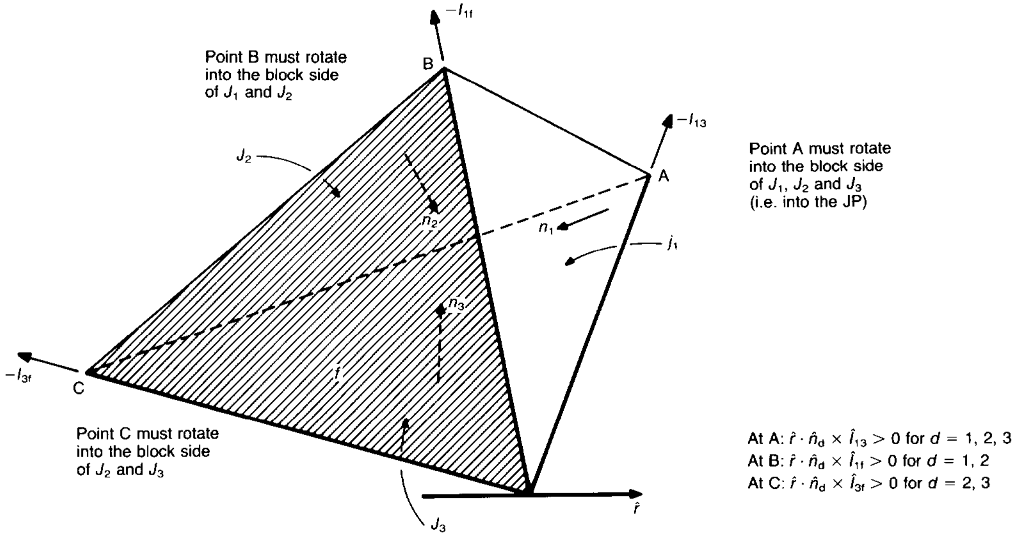

Fig. 46. Rotational kinematics for rotation about an axis intersecting a corner on edge I_{13} (after Mauldon, 1992a)

about an axis in corner I_{ij}, the direction of the axis is constrained by the seven inequalities to lie in the shaded spherical quadrilateral. Then a series of trial moment calculations for a range of axis directions in this solution space is sufficient to assess the rotational stability for the selected corner.

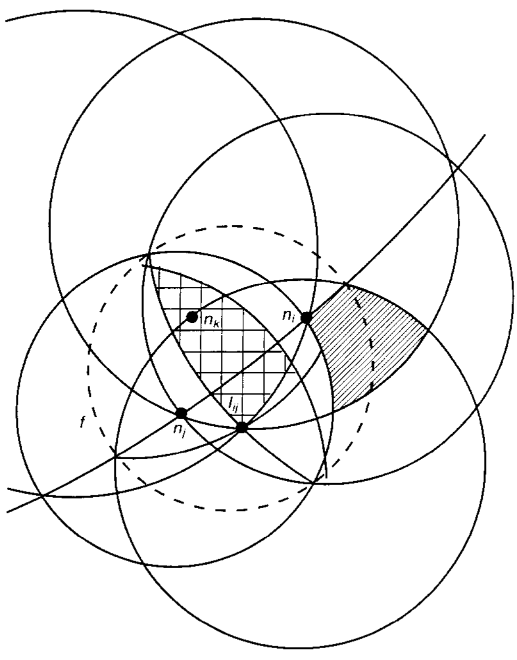

Fig. 47. Restricted range of axis orientations that are kinematically possible for rotation about corner I_{ij}, based on the inequalities in Fig. 46

Relative importance of rotational modes

Although the discussion of rotational block theory may seem complex, the steps are tractable and the analysis can be conducted as part of an engineering design study. Such analyses are not usual. This cannot be correct because a comparison of the stability regions for sliding and rotational equilibrium shows that rotational modes may be unstable for a block which is otherwise demonstrably stable against sliding. To appreciate this one has only to consider the case where the friction angle is 90° on each plane. In this case all the reference sphere outside the JP is safe from sliding. However, the friction angle is not contained in the construction of the median plane for rotational equilibrium and there will, in general, be regions of rotational disequilibrium even with these high friction angles.

In general, high joint shear strength promotes rotational movements. This comes about when there are steep asperities adding a high roughness angle to the basic joint friction angle. Even one orthogonal step in a joint face can prevent sliding. However, these steps would not necessarily inhibit rotational movement, which may be directed normal to the joint surface, as shown in Fig. 48. Furthermore, because rotational movement tendencies produce virtual displacements normal to joint surfaces, they can reopen previously healed joints and liberate new blocks. Rotational movements form kink bands in direct

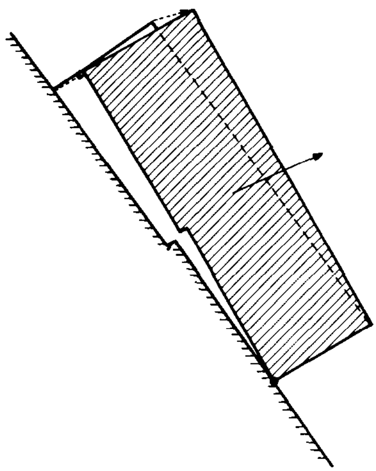

Fig. 48. Incipient motion direction in rotation can overcome steep asperities that would prevent translational shear failure

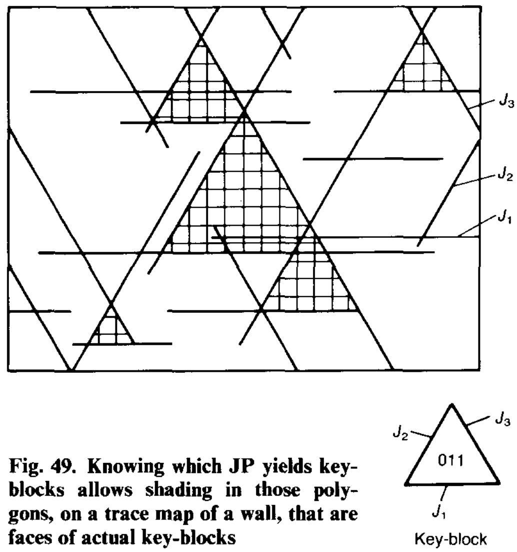

Fig. 49. Knowing which JP yields key-blocks allows shading in those polygons, on a trace map of a wall, that are faces of actual key-blocks

shear specimens with inclined layers when the roughness is such that sliding is restricted.

A block that is at rest in a static, dry condition may become unstable during an earthquake or storm due to rotation of the resultant force away from the vertical. Even modest water pressures on the face of a block are capable of rotating the resultant a long way from vertical. If the joint has a high shear strength due to steep roughness or unjointed rock bridge segments, the block will not be able to slide, although it may be able to rotate. I believe that this mechanism is active and accounts for landslides and rock falls after rains and earthquakes.

PROBLEMS THAT CAN BE SOLVED USING BLOCK THEORY

Block theory can help to find solutions for a number of design problems. Among these are questions of assessing the safety of rock foundations with potential rock blocks, estimating probable support requirements for tunnels, finding the minimum safe separations between parallel tunnels or drifts, evaluating the effect of tunnel or shaft size on the cost of support, determining the lengths of rock bolts to assure anchorage behind key-blocks of tunnels and chambers, and predicting the most stable orientations for a shaft or tunnel.

Identifying and analysing actual blocks in foundations

During the construction of major foundations, such as those for a large dam or powerplant, trace maps can be prepared for the exposed walls. From these, all potential key-blocks can be located for timely treatment. However, before rock faces have been exposed, it may not be possible to acquire such specific data; in this case, rock trace maps can be simulated repeatedly for a Monte Carlo type analysis, using block theory to find the key-blocks from each trace map realization to test the relative adequacies of a series of trial designs. The problem posed by safety analysis of an existing structure is intermediate between these extremes, with specific but incomplete data available from construction photographs or logs, or acquirable from partial exposures.

When a trace map is acquired for the foundation surface, it is possible to locate the faces of all removable blocks. The different joint traces cut a large number of polygons, each of which might be the face of a key-block or potential key-block. Block theory identifies the JPs that are potential or real key-blocks. Each produces a particular shape of polygon on the face in question. Locating the actual removable blocks is then a simple problem in pattern recognition, which can be solved manually or with the aid of a block theory program.* Fig. 49 presents a simple example. Knowing that the JP code for the potential key-blocks is 011, the squared regions establish the potentially dangerous faces.

A recent example from engineering practice is a safety evaluation performed for the US Bureau of

* A series of programs for the application of block theory were written by Gen Hua Shi.

Reclamation's Seminoe arch dam—a 90 m high slender structure built in the late 1930s in a steep Wyoming canyon cut in blocky pre-Cambrian granite (Goodman & Scott, 1994). Joint traces were well-exposed on the walls of the canyon but very few data were available on traces in the footprint of the dam. The safety of the dam was being appraised in consideration of hypothetical extreme flood flows and/or a severe earthquake. Two types of analysis were made.

First, the joint system was characterized from the separate data sets for the right and left canyon walls, and the removable blocks of the upstream and downstream abutment areas were drawn on planes tangent to these walls. Scanning for patterns in the trace maps of the walls similar to these drawings revealed a number of candidates for stability analysis.

Second, all polygons on the trace map were numbered and the half space combination (JP) describing each polygon was determined; a search was then made through the long list of JPs to find which were removable in the local space pyramid. Rather than using a single nominal orientation for each joint set, this procedure incorporated the orientations of the actual traces forming the particular faces.

The joint pyramid of any block found to be removable by either procedure then received a stability analysis; this produced a short list of blocks for which the friction angle required for equilibrium was higher than the conservatively selected figure of 10°. It was believed that all joints and faults at the site produced friction angles considerably higher than 10°.

A plan view was drawn for each block on the short list, using the surface joint traces plotted on a topographic map. Some of these blocks were seen to continue under the footprint of the dam. The weights of the block and the water forces were calculated; static and dynamic structural loads were added from the results of dynamic finite element analyses previously conducted by the Bureau of Reclamation for various load cases. Finally, the design earthquake for the bedrock was imposed and the increments of displacement were computed for the temporally appropriate mode resulting from each pulse. This analysis was repeated for a range of friction angles to determine the particular value of the friction angle required to keep the cumulative displacement satisfactorily small. This mobilized friction angle was compared with the friction angle believed to be available in the rock joints. Fortunately, all blocks were found to be sufficiently safe.

Figure 50 shows the largest and most critically placed of the potentially significant blocks. The results of the dynamic calculation are shown in Fig. 51, from which it was judged that the block was not a danger to the dam if the friction angle was greater than about 31°, and this was judged to be acceptable for this block. Had it not been,

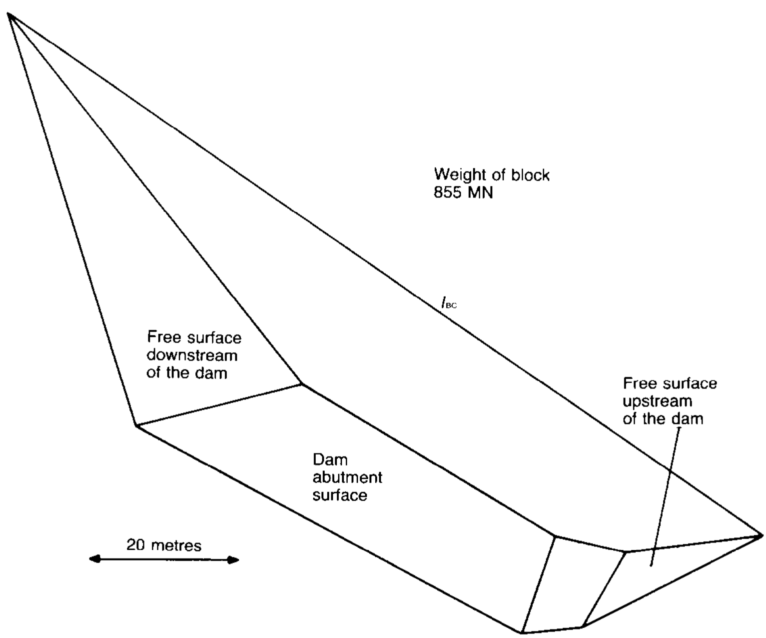

Fig. 50. Potential key-block identified in foundation of Seminoe Dam

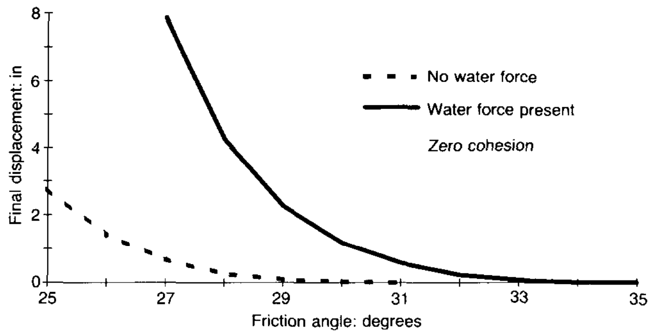

Fig. 51. Results of dynamic analysis of the potential key-block in Fig. 50

field testing or structural work would have been initiated.

A similar analysis was conducted for the abutments of Pacoima Dam, Los Angeles County—a 112 m high arch dam flood control structure built in 1929—in consideration of alternative spillway enlargement schemes.* One apparently cost-effective alternative was to augment the existing spillway discharge with an additional chute that would produce flows impacting the left abutment. The abutment is composed of blocky, foliated granite with platy schistose zones. The abutment rocks had been coated with pneumatically applied mortar, which masked the traces of most fractures. However, many fracture traces showed on construction photographs and some were shown on geological maps. Also, important individual traces and the moulds of a number of displaced blocks showed cleanly through the gunite cover. Analysis of the jointing directions revealed strongly preferred orientations in at least three extensive sets and the application of block theory to this system established the riskiness of endangering the left abutment with impacting water jets.

The application of block theory to the free faces of the right abutment showed fewer potential key-blocks. Few moulds of displaced blocks could be found there, which suggested that this abutment was more stable. Unfortunately, few traces of joints showed through the gunite mantle or on the construction photographs. Accordingly, trace maps were simulated using a stochastic method.

A number of engineers have developed models to simulate joints in a rock mass. A jointed rock mass can be represented as a very large volume with an almost infinite population of finite flat

* Work performed jointly with Y. Hatzor for Dames and Moore on behalf of the Los Angeles County Department of Public Works.

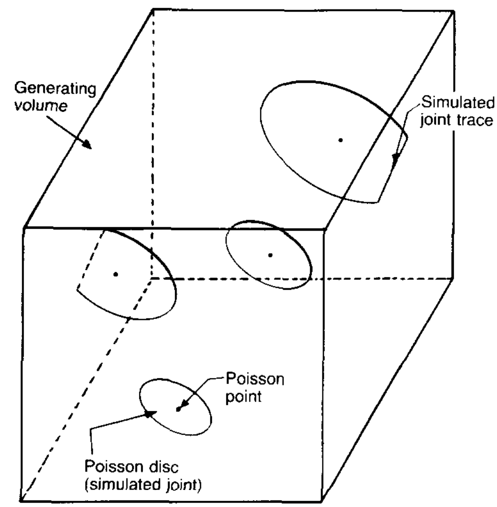

Fig. 52. Method of simulating joint traces on an excavation surface using the Massachusetts Institute of Technology Poisson disc model

joints centred randomly throughout the volume. Using the Poisson disk model of Baecher *et al.* (1977), Chan & Goodman (1983) developed a program to insert joint disks of fixed orientations randomly to simulate particular distributions of spacing and extent, and computed the traces of intersection of this system on a specified rock excavation plane. Fig. 52 shows this approach. Unfortunately, it proved impractical to select a sufficiently large generating volume because the most important joints are long. This barrier may now be moot, with the development of powerful three-dimensional joint simulation programs for hydrogeology (e.g. FracMan software offered by Golder Associates, Seattle (Dershowitz, Lee, Geier, Hitchcock & LaPointe, 1995).

The simplified trace map simulation technique used here, from Shi, Goodman & Tinucci (1985), assumes joints of determined orientations in *n*

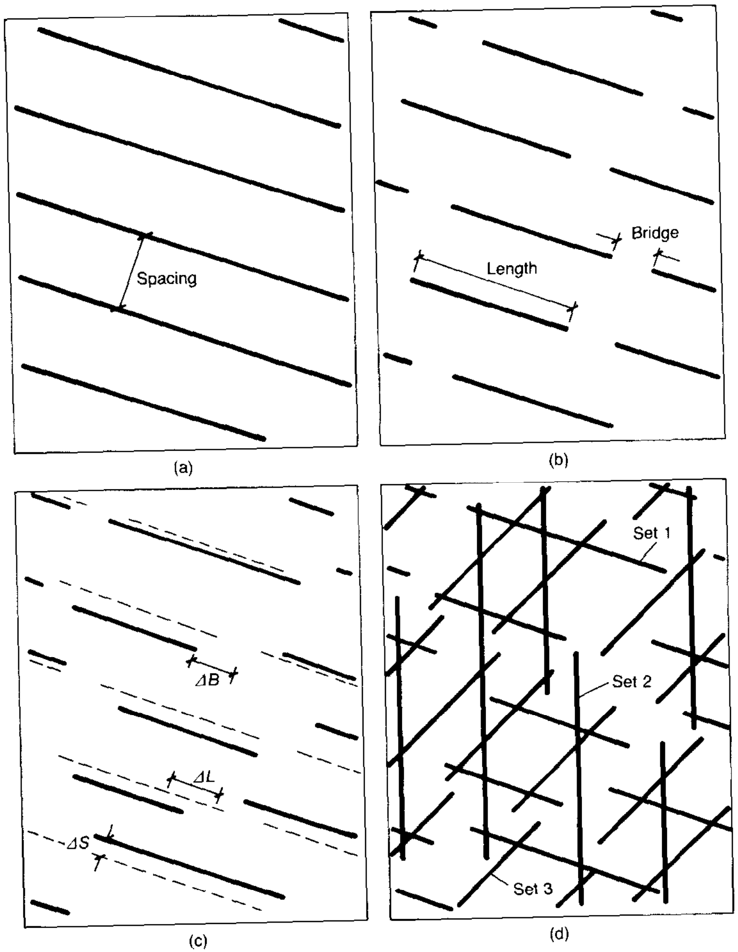

Fig. 53 (left). Shi's method for simulating joint traces on a plane excavation surface

Fig. 54 (below). Key-blocks of the right abutment of Pacoima Dam: (a) joint traces simulated in one realization; (b) corresponding key-blocks

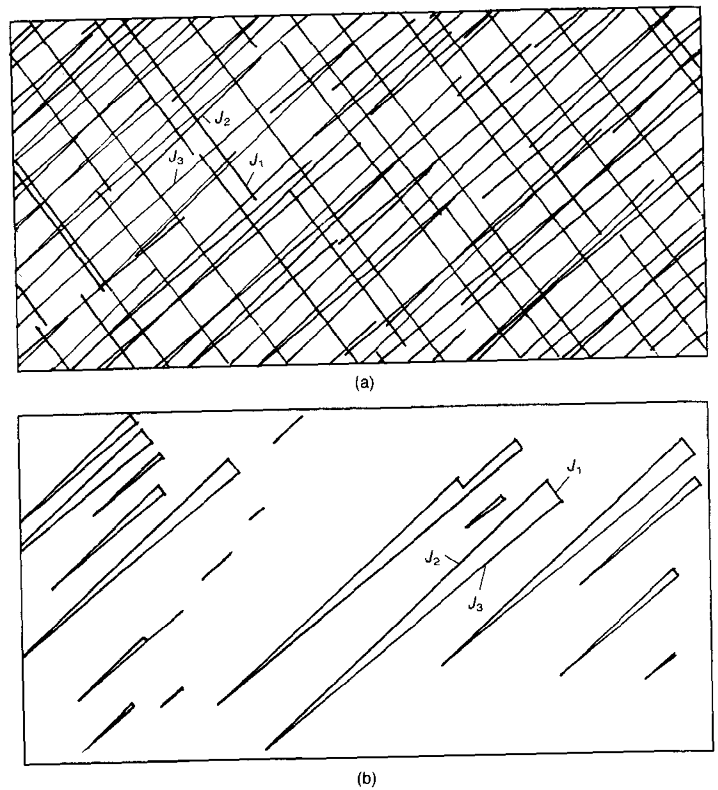

sets. Each joint set begins life as a regular, infinite ruling of traces at fixed separation across the excavation surface, as shown in Fig. 53(a); these are then broken, as in Fig. 53(b), and moved without rotation by small distances to achieve random segment lengths, random spacings and random bridge distances between the end of one joint and the start of the next (Fig. 53(c)). The degree of randomness is specified with the input. The perturbed joint traces intersect to form polygons (Fig. 53(d)) whose stability is established using the methods described.

In the case of Pacoima Dam, the block simulations on the right abutment, represented by the realizations in Fig. 54(a), showed that it was not possible to encounter important key-blocks like those in the left abutment. The likely key-blocks instead were shallow, insignificant wedges like those in Fig. 54(b). It was decided to construct a new supplementary chute spillway on the right abutment, with the discharge conducted to avoid spillage against the left abutment. The chute excavation will be rock bolted, the bolt design being adjusted sensitively to blockiness revealed during construction. The state gave its approval to this scheme, provided there was close inspection of the geology and reassessment of the blockiness during the construction.

Finding the maximum key-blocks of tunnels

In his Rankine Lecture, Ward (1978) stated

> Tunnel construction is decidedly a three-dimensional operation and discontinuities certainly need to be considered in three dimensions to understand their influence on the safety and instability of tunnel excavations, and on support needs.

He made convincing use of three-dimensional block models to communicate tunnel block possibilities to others. Here I show how block theory can be used in different aspects of the tunnel design problem.

A cylindrical excavation is the space common to the intersection of free surfaces parallel to the

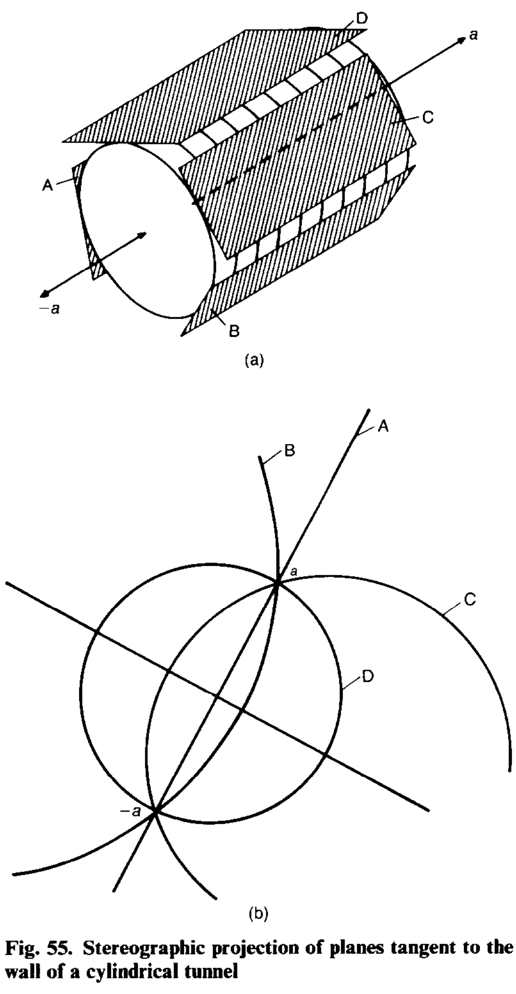

Fig. 55. Stereographic projection of planes tangent to the wall of a cylindrical tunnel

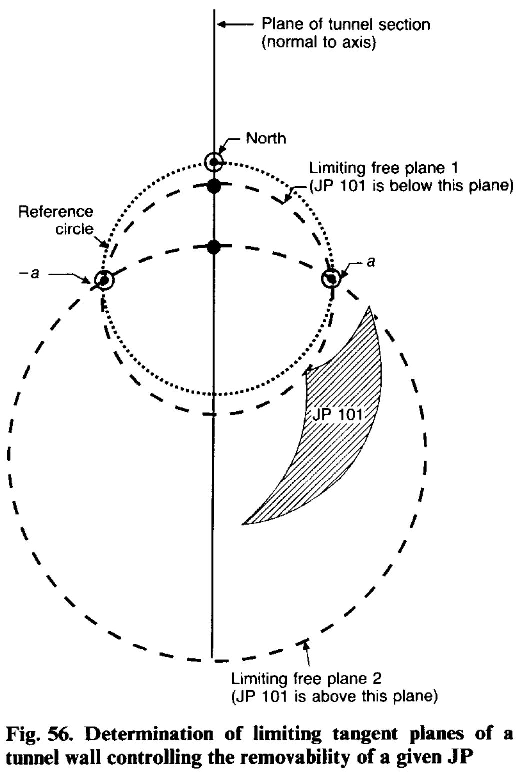

Fig. 56. Determination of limiting tangent planes of a tunnel wall controlling the removability of a given JP

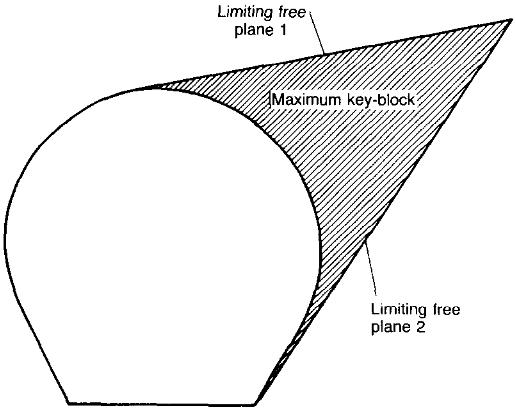

Fig. 57. Determination of the location and area of the maximum key-block of a tunnel for a given JP, corresponding to the construction of Fig. 56

tunnel axis *a*. A joint pyramid that contains this axis is not removable from the walls but every other joint pyramid has removability in some region of the tunnel walls.

The tunnel walls contain an infinite set of tangent planes through *a*, as in Fig. 55(a) where four such tangent planes have been selected arbitrarily. These planes project in the stereographic projection as a family of great circles through *a*, the four illustrative individuals of Fig. 55(a) being represented as shown in Fig. 55(b). If a tangent plane great circle is constructed to pass very near to an extreme corner of a selected joint pyramid that does not contain the tunnel axis, one half space of that great circle will completely contain the JP. Therefore the selected JP is removable in an excavation parallel to the constructed great circle such that the space pyramid is on the JP side.

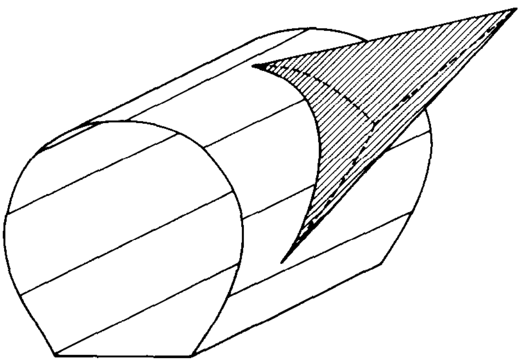

Fig. 58. Actual three-dimensional key-block corresponding to the projected maximum key-block area in Fig. 57

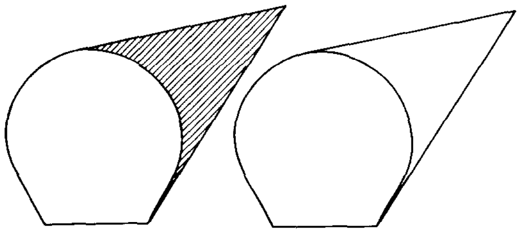

Fig. 59. Use of the maximum key-block areas to find safe separation of parallel tunnels in order to assure survival of the wall pillar

Repetition of this construction by trial for the other corners of the JP produces one additional limiting free plane tangent to the wall such that the JP is removable in one of its half spaces. As shown in Fig. 56, the intersections of these limiting tangent planes with the plane normal to the tunnel axis determine the traces of the limiting planes as seen in the tunnel cross-section. These traces are drawn tangent to the tunnel such that the JP is on the correct side of each, as shown in Fig. 57. The two tangent lines thus drawn in the tunnel section delimit a pie-shaped region; the vertex of the hat lies at a determined point inside the tunnel wall. This is the maximum key-block region for the selected JP, previously identified in Fig. 12. Its area is A_{mkb}.

The construction for the traces of the maximum key-block region in the tunnel section is exactly the same as the construction for the orthographic projections of the edges of the JP in the tunnel section, i.e. the maximum key-block region is formed by projecting the lines of intersection of joint planes into the tunnel section.* The real key-block is a three-dimensional curved wedge, oblique to the tunnel, as shown in Fig. 58.

Having determined the maximum block size corresponding to a given JP, the mode and stability analyses can be used to find the most critical blocks of the tunnel, both with respect to sliding and rotation. Moreover, the known radial distance to the vertex of the maximum key-block for each JP reveals the minimum free length of rock bolts to assure anchorage behind the key-block zone.

Finding the safe separation of parallel tunnels or shafts

The pillar of rock between parallel openings must not suffer dangerous loss of integrity from

* The traces of the key-block region in the tunnel section are frequently assumed, in error, to be formed as intersections of the plane of the section with the joint planes; such traces would pertain to stability of the tunnel face, but not to stability of the tunnel walls.

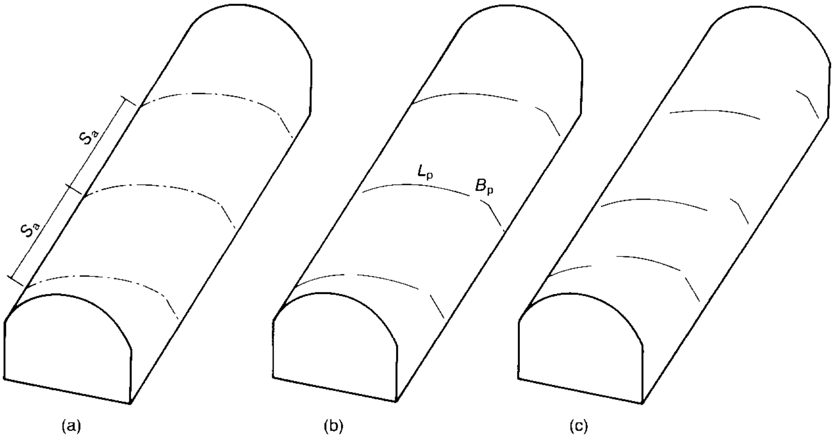

Fig. 60. Shi's method of simulating joint traces applied to generating trace maps on a tunnel interior (compare with Fig. 53)

block sliding. The maximum key-block regions indicate the maximum extent of initial block movements that could be caused by the loss of a maximum key-block from each side of the wall pillar (Fig. 59). This would still be an insufficient thickness if the movement of a key-block into either opening were allowed to precipitate a progressive failure involving additional blocks.

Estimating the real key-block regions

The maximum key-block regions determined by the limiting tangent planes as described were based on the assumption that the joints are infinite in extent. If this is not the case, or if actual joint traces can be observed, the tunnel support can be effected more economically with smaller probable key-blocks. This analysis requires simulation of joint traces through the region of the tunnel. The simulation can be assigned a greater degree of confidence if it is able to incorporate the joint traces mapped in a pilot tunnel or in neighbouring tunnel sections.

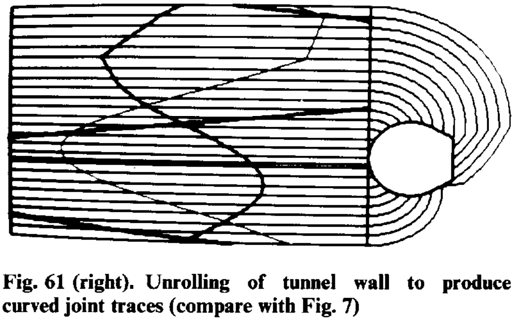

Fig. 61 (right). Unrolling of tunnel wall to produce curved joint traces (compare with Fig. 7)

The method of joint simulation discussed for Pacoima Dam has been applied to this problem. A set of regular joint planes generally oriented relative to the tunnel produces a set of oblique loops on the tunnel periphery (Fig. 60(a)). These are perturbed to produce randomly varying trace length, spacing and bridge distance (Figs 60(b) and 60(c)). Repetition for each of n differently oriented joint sets produces intersecting, oblique finite traces on the tunnel walls. The tunnel is unrolled from a selected cut point (Fig. 61), producing curved joint traces like those noted in actual tunnel and borehole logs (compare with Fig. 7).

Each simulation of joint traces yields a developed drawing like Fig. 62 in which the intersections of traces yield many polygons, only some of

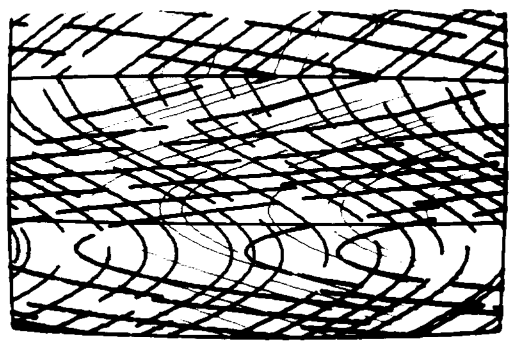

Fig. 62. Curved traces resulting from application of the method of Fig. 60, and consequent unrolling; the horizontal lines delimit the area of the maximum key-block for a particular JP

which are the faces of removable blocks. For the tunnel case, working with unrollings of the tunnel walls, the polygons have curved sides. Even so, block theory identifies the removable blocks, using efficient computer programs by Gen Hua Shi to draw all the loops that enclose nesting, non-convex removable blocks corresponding to each JP. For a given JP, the developed view can be reduced to a smaller rectangle corresponding to the section of the wall between the tangent lines of the JP's maximum key-block, as determined by the limiting free planes (Figs 56 and 57). Then each realization of the simulation process results in a map of key-block faces like that in Fig. 63.

The stability analysis of the JPs in the tunnel determines which are the most significant key-blocks, and the unrolling procedure determines their area of intersection on the tunnel periphery.

In a recent development, Shi has developed a program used by Chern & Wang (1993) to determine the volumes and the radial distances from the tunnel wall to the various vertexes, of the nesting, united real key-blocks. The procedure used to do this is as follows. Having established the simulated joint traces, a series of progressively larger over-cylinders is drawn, each one yielding a map of key-block faces like that in Fig. 63. As the over-cylinders expand outwards, the key-block faces shrink and eventually disappear. The radius of the cylinder that causes virtual disappearance of a key-block region establishes the radial distance to its vertex and when all such faces have disappeared from the unrolled view, the largest such key-block has been measured. Moreover, the family of shrinking key-block areas determines the complete three-dimensional geometry of these regions. Fig. 64 shows the faces of the key-blocks for three intermediate enlargements; the fact that these faces shrink as the unrolled cylinder enlarges proves that block theory has correctly identified these faces as belonging to removable blocks.

The method of successively enlarging cylinders can also be used to interpret actual trace maps recorded on tunnel walls. This is particularly applicable for machine-bored tunnels, which provide a clear image of the joint traces.

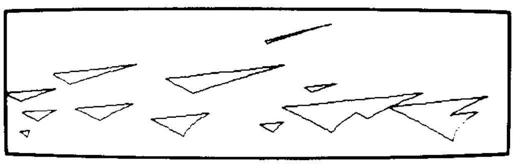

Fig. 63. Faces of key-blocks corresponding to the selected JP for the particular trace simulation

The use of block theory and joint simulation for tunnels makes it possible to examine the relative costs of tunnelling in a given rock mass with different sizes and shapes of tunnel cylinder. The effect of tunnel size is striking: as the tunnel is enlarged, in a given blocky rock mass, not only are the key-block regions correspondingly enlarged, but also the real key-block areas on the walls increase disproportionately, and eventually fill the entire maximum key-block regions. As the key-block areas increase, so do the radial distances to the vertexes, but they can never be larger than that of the maximum key-block.

As overbreak tends to empty portions of the maximum key-block regions and the extent of these regions is sensitive to the tunnel shape, the extent of overbreak and rock loosening can be reduced by optimizing the tunnel shape. This assumes that the rock mass traversed by the tunnel can be characterized by a stationary set of joint orientations. Such economies cannot be established in a rock mass with a joint system which varies widely along the length of the tunnel.

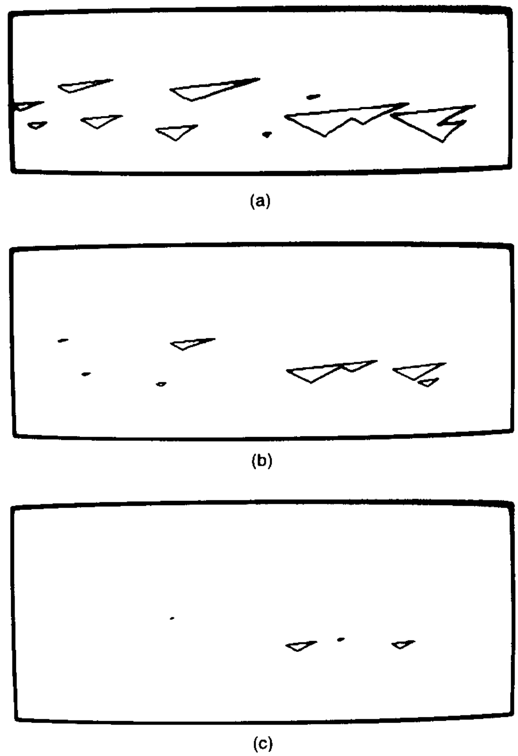

Fig. 64. Reduction of the key-block areas for the selected JP on successively larger over-cylinders

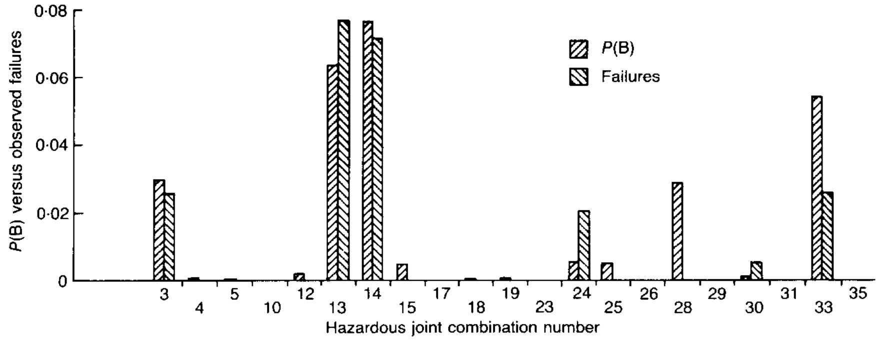

Fig. 65. Hanging Lake tunnels: comparison of Hatzor's key-block likelihood parameter with the relative number of block failures involving different joint set combinations

Finding the design block for real joint systems

Some blocky rock masses embrace only strongly clustered joint orientations that are well characterized by three non-dispersed joint sets. The nominal joint orientations for these sets can then be used with block theory in a pseudo-deterministic analysis of a repeatedly jointed rock.

In other cases, as at Seminoe Dam, particular subsets of joint individuals are identified and analysed; although the faces of the potential block being studied are probably not perfectly planar, a single nominal orientation is introduced for each face in what is truly a deterministic problem.

More complex problems are usual in granitic and metamorphic rocks. For example, the joint attitudes in migmatitic gneiss and quartz diorite measured in the pilot tunnel for the Hanging Lake highway tunnels in Glenwood Canyon, Colorado* are a dispersed system of directions that can be clustered into at least seven distinct, but scattered, sets. Choosing nominal directions for each of these provides input for block theory. Seven joint sets can combine to produce a large number of JPs (seven joint sets can combine in subsets of three or more in 99 different ways) so that the practicality of the method is called into question. However, it proves feasible to reduce the problem to manageable size by preferring only those combinations that are most likely.

The relative likelihood of different combinations of joint sets (JCs) was studied by Hatzor (1992) who described blocks that had formed in the pilot bore and then in the final excavation of the Hanging Lake tunnels. A significant simplification became evident on plotting the different JCs representing 35 blocks that had dropped out during construction of the pilot bore: 33 of these were formed of three joint sets, two were formed of four joint sets and none were formed of five or more joint sets or involved blocks with parallel joint faces. Only one block involved a new fracture induced by the excavation. In an inspection of a section of the full-size tunnel during construction, 34 additional block failures were studied, all of which involved JPs with three joints.

The fact that most blocks in the Glenwood Canyon tunnels had JPs with only three of the joint sets, despite the existence of seven joint sets in the rock mass, is to be expected. The joints forming a single block must coexist in the volume of that block. The likelihood that joints of different sets will pass through a given small volume of rock depends on the product of the relative frequencies of the joint sets.* The probability of a fourth joint crossing a volume near the intersection of three joints is less than the probability that the original three joints will intersect.

As a simplification, therefore, it can be recommended that the most likely blocks will be formed of JPs from combinations of three joint sets. However, as a larger number of joints in the JP may facilitate rotational failures, this does not assure that the most hazardous block will not be one with more than three joints. A full analysis requires attention to all possibilities.

Among the many combinations of n joints taken three at a time, it is possible to apply weighting factors to express both their relative likelihood and the degree of hazard that they cause in a particular surface or underground excavation. This approach was used by Hatzor & Goodman (1992a) to analyse the blocks of the Hanging Lake tunnels; they drew on formulations by Mauldon (1990, 1992b) and Shi *et al.* (1985) to express an approximate block failure

* Geotechnical work by Woodward Clyde Consultants Inc.

* Joint frequency is the mean number of joints per unit of distance in the direction normal to the joint.

likelihood function. Fig. 65 compares this likelihood function with the numbers of block failures that were mapped in a section of the full-sized bore for each of the 35 different combinations of three joint sets. It can be seen from this comparison that it is possible to predict which combinations of joint sets will be the most likely to produce block failures.

The application of the block failure likelihood function in the Hanging Lake tunnels identified not only the joint combinations, but also the actual JPs that caused most of the block failures. In the pilot bore, 60% of the block failures were produced by the key-blocks of only two joint combinations; those joint combinations tagged by the block failure likelihood function as being most critical accounted for 76% of all block failures. Furthermore, joint combinations identified from the analysis as being safe were absent from the record of actual block failures. In the section of the full-size bore studied during construction the results were similar, with the key-blocks of three joint combinations accounting for 84% of the failure cases; joint combinations identified as critical accounted for 90% of all block failures. In this case one failure case was attributed to a joint combination that had been considered to be safe; this individual involved specific joint attitudes which were removed from the nominal set orientations and shows the hazards of over-simplification when characterizing dispersed joint sets.

The likelihood that a particular combination of three joint sets will produce a dangerous key-block in a particular excavation depends on

(*a*) the probability that the three joint sets will intersect near the excavation
(*b*) the probability that their point of intersection is such that the resulting block will be removable in the excavation
(*c*) the degree of instability of these removable blocks.

Assuming joints of infinite extent, the probability that three particular joint sets will intersect depends on their orientations and average frequencies. The probability that their intersection will be located such that the resulting block is removable depends on the size and shape of the excavation and its orientation relative to the joint sets. For sliding modes, the degree of instability depends on the steepness of the sliding surfaces and the friction angles for a given JP. (Rotational modes are not included here.)

Mauldon (1992b) derived expressions for the probabilities involved and assembled these relationships to express the expected value of the maximum support force E_{msf} of any JP that might intersect a tunnel

$$E_{\mathrm{msf}} = [\lambda_i \cdot \lambda_j \cdot \lambda_k \,|\, n_i \cdot n_j \times n_k \,|\, A_{\mathrm{mkb}} F_{\mathrm{s}}] \qquad (2)$$

where λ_i is the average frequency of joint set i, and so on, and n_i is the normal to joint set i, and so on.

A_{mkb} is the area of the maximum key-block for the particular JP of the joint combination i, j, k. For a tunnel, it is the region of the maximum key-block in the tunnel cross-section as shown in Fig. 57.

F_{s} is the sliding force for the JP in the particular tunnel. The sliding force is the difference between the new downslope force on the block and the total frictional resistance. It is positive for an unstable block and negative for a stable block.

Equation (2) can be used to compare tunnelling support costs in different orientations through a rock mass. For the present purpose, in finding the most critical joint combinations and their key-blocks, it is preferable to replace the sliding force with a simplified index. Hatzor's (1992) instability parameter varies between 0 and 2 as the sliding condition of a block changes from completely safe to completely unsafe (with the limit of equilibrium at a value of the index equal to unity). Introducing an expression from Hatzor & Goodman (1992a) in place of F_{s} defines the block failure likelihood L_{bf} as

$$L_{\mathrm{bf}} = [\lambda_i \cdot \lambda_j \cdot \lambda_k \,|\, n_i \cdot n_j \times n_k \,|\, A_{\mathrm{mkb}} 2^{(F_{\mathrm{s}}/W)}] \qquad (3)$$

where W is the weight of the key-block. (F_{s}/W is independent of size for purely frictional joint strength.)

The joint combinations with the highest values of the block failure likelihood are those that are most critical for design, and their key-blocks determine a manageable number of design blocks. This provides a practical way to use block theory even when the number of joint sets is large. However, when the joint sets are poorly defined because of large dispersion of the joint orientations, the possible errors in using the design block would have to be evaluated a priori.

Predicting optimum directions for tunnelling or shafting

Assuming that a rock mass to be tunnelled can be characterized throughout by a single system of joints, it is possible to choose a most stable direction for tunnelling. For a defined tunnel or shaft axis, each joint pyramid that contains the tunnel or shaft axis has a maximum key-block region with area A_{mkb} specifically located in the tunnel walls. (The methods of making this determination are shown in Figs 56 and 57.) Stability analysis for the key-blocks occupying this region determines a minimum support force required for a given degree of safety. For simplicity and consistency the support force can be applied in a radial direction and the factor of safety can be taken as unity.

In the absence of particular information about joint spacings, the whole of each key-block region is multiplied by the rock density to determine the weight of maximum key-block per unit length of tunnel from which is calculated the maximum key-block support force per unit length of tunnel. (This procedure corresponds to assuming that the joints are infinitesimally spaced.) The largest support force per unit tunnel length of any key-block of any combination of three joint sets is accepted as the support force characteristic of that tunnel or shaft direction.

If the joint spacing is finite, and presumably different for the different joint sets, the expected value of the support force for the given tunnel or shaft direction can be calculated using equation (2). The term A_{mkb} is part of the formulation for the relative probability of occurrence of the key-block and is used independently of the sliding force. Thus the use of equation (2) involves a variation of support force with the square of the maximum key-block region. Rather than taking the maximum value of E_{msf}, it is appropriate to sum all the values of E_{msf} for each JP of each joint combination (Mauldon, 1992b).

Repetition of either procedure for the full range of directions in space yields a field of support loads corresponding to all possible tunnel or shaft directions.

Such a result is shown in Fig. 66, in which the relative support requirements for tunnelling or shafting in different directions have been contoured on the stereonet. The orientations having low contour values will be most desirable with respect to tunnel support costs. The support load contour diagram and the expected maximum support force are both system properties that depend on joint orientations and friction angles as well as tunnel shape. However, if the tunnel shape is maintained constant, the variations are exclusively a function of the rock mass properties and the diagram can be considered to be an attribute of the rock mass.

When the excavation direction analysis has been restricted to finding the azimuths of horizontal tunnels, results typically record one or two directions of anomalously higher support needs. When plotted in a Cartesian space with the tunnel azimuth as abscissa and the support force as ordinate, such a diagram can resemble a spectrum. Hence the plot of tunnel support force versus tunnel direction has been called the tunnel support spectrum. Similarly, Mauldon (1992b) called a plot of the expected value of maximum support force versus tunnel direction, as in Fig. 67, the probabilistically weighted tunnel support spectrum.

Mining engineers interested in planning layouts for caving methods of mining may be tempted to use the contour highs on the support load diagram as directions for development drifts. However, as stated at the outset, this analysis does not predict whether or not caving will occur in such drifts but only that they would remain stable if the key-blocks were supported.

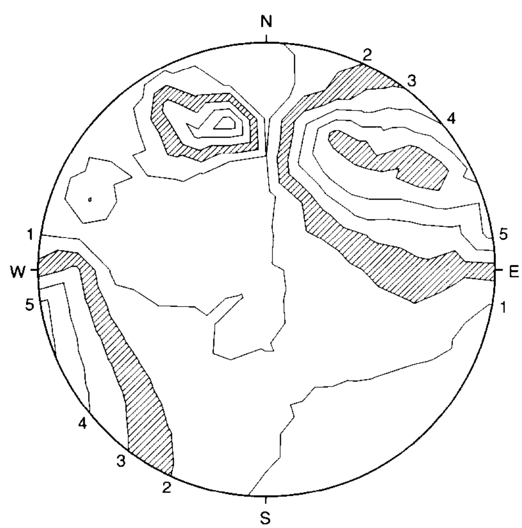

Fig. 66. Relative support requirements for different directions of tunnels and shafts with respect to block stability

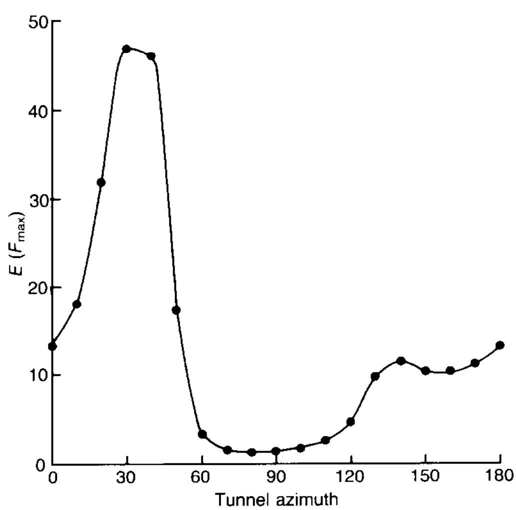

Fig. 67. Expected value of the maximum support force for a given joint system intersecting horizontal tunnels driven in different directions (after Mauldon, 1992b)

The three-foot rule

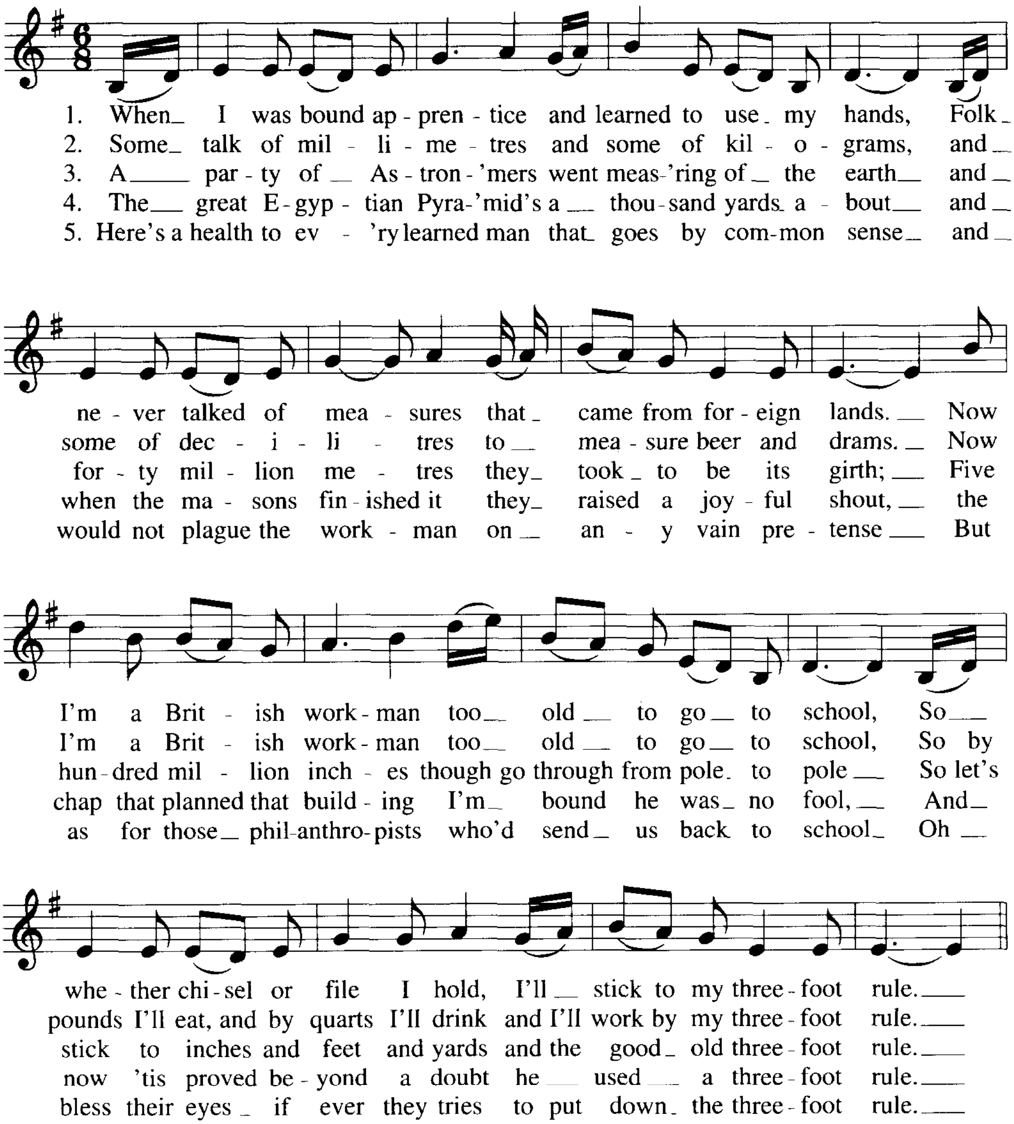

6. The times now are quite different: we've learned the metric scale,
And workers in Great Britain are at one with fax and 'E-mail'
So might the British soils man, too old to go to school,
Abide the laws that give good cause to adopt a 3-d rule.

Fig. 68. ***The three-foot rule*** **by W. J. M. Rankine, with the addition of a sixth verse**

CONCLUSIONS

Blocky rock masses can deform by virtue of the general movements of component blocks. Block theory facilitates calculation of the many degrees of freedom by focusing on key-blocks. Support of all key-blocks, according to the fundamental axiom of block theory, guarantees stability for the rock mass. Pioneering analyses by Londe *et al.*, (1969, 1970), Wittke (1984) and John (1968) provided the basis for stability analysis. Block theory places this work in a larger kinematic context and provides computational tools that underpin complete analysis of large and highly jointed rock masses.

Many types of rock mass are not amenable to analysis by block theory, so the methods described here are only one set of tools needed by the engineer. In any event, the engineer can make good use of complementary tools that help describe and quantify geometric and mechanical properties of the system of discontinuities—particularly stochastic methods because discontinuities are statistical in nature. Fortunately this is a subject that the field of rock mechanics has addressed vigorously.

Among the attributes of blocky rock masses that affect the style and substance of engineering analysis, directionality of properties and behaviour is perhaps the most important. This dictates a necessary measure of three-dimensionality in many real problems. Methods that do not facilitate computations in three dimensions are less preferable than those that do. Also, for specific questions that merit individual study, it should be preferable to attempt specific structural analyses whenever the requisite geological information can be acquired.

Among the behaviour of rock blocks is a variety of failure modes involving rotation or rotation combined with sliding. It has been shown that foundation blocks that are safe from sliding may be unsafe in rotation. Rotational modes are favoured by high joint friction angles as, for example, when the roughness includes very steep asperities or steps, or when the potentially failing block is not completely isolated by continuous joints so that some rock breakage or reopening of healed joints has to precede failure. Rotational modes can be engendered under gravity alone but particularly when the direction of the resultant force is rotated away from the vertical by inertia forces or water pressures on the faces of rock blocks. Methods were introduced for analysing rotational modes of failure—particularly for tetrahedral blocks with three non-parallel joint faces.

Many of the engineer's questions about rock behaviour can be addressed using block theory. These include scale effects in tunnelling, the design of portals and intersections of tunnels, and the selection of optimum tunnel or shaft orientation and shape. Water forces on dam foundations and abutments and in rock slopes can be introduced and are often vital to the understanding of rock behaviour.

The idea of calculating rocks based on a design block brings block theory to immediate applicability in many kinds of engineering calculations. The design block can be taken as the largest possible key-block of an excavation but this would be over conservative in many instances. Probabilistic methods can increase efficiency in rock engineering designs by providing a more realistic basis, although this will not be without some jeopardy—hopefully small—because the maximum key-block does occasionally materialize, particularly in surface excavations.

Although the methods discussed in this lecture may seem complex, they are based on simple geometric and logical precepts and can be mastered, and applied in the real world of engineering practice. I have no illusions, however, that hordes of geotechnical engineers and geologists will quickly fly towards their adoption, any more than Professor Rankine had illusions that British workers would fly to embrace the metric system. In fact, he wrote a song to that effect (Rankine, 1874) called *The three-foot rule* (Fig. 68), which I shall now sing to you.

ACKNOWLEDGEMENTS

I am deeply indebted to the British Geotechnical Society for their having afforded me the privilege to present this Rankine Lecture, and also to Dr J. Hudson and Dr M. de Freitas for their generous comments.

My work on block theory has benefitted from the collaboration of a number of creative people to whom I am indeed grateful, chief among them being Dr Gen Hua Shi. Professor M. Mauldon, and Dr J. Kuszmaul, Professor Y. Hatzor, Dr Lap Yan Chan, Dr B. Thapa, Dr A. Bro, Dr A. Karzulovic, Dr W. Boyle and Dr J. Yow are also thanked.

My work on block theory has received financial support from the California Institute of Mining and Mineral Resources Research, and the National Science Foundation, as well as funding for specific applications from the Defense Nuclear Agency, the US Bureau of Reclamation, Dames and Moore, and the Los Angeles County Department of Public Works.

Finally I am indebted to the Norwegian Geotechnical Institute for gracious assistance with the final preparation of a number of figures.

APPENDIX 1

The stereonet shown here is useful for block theory.

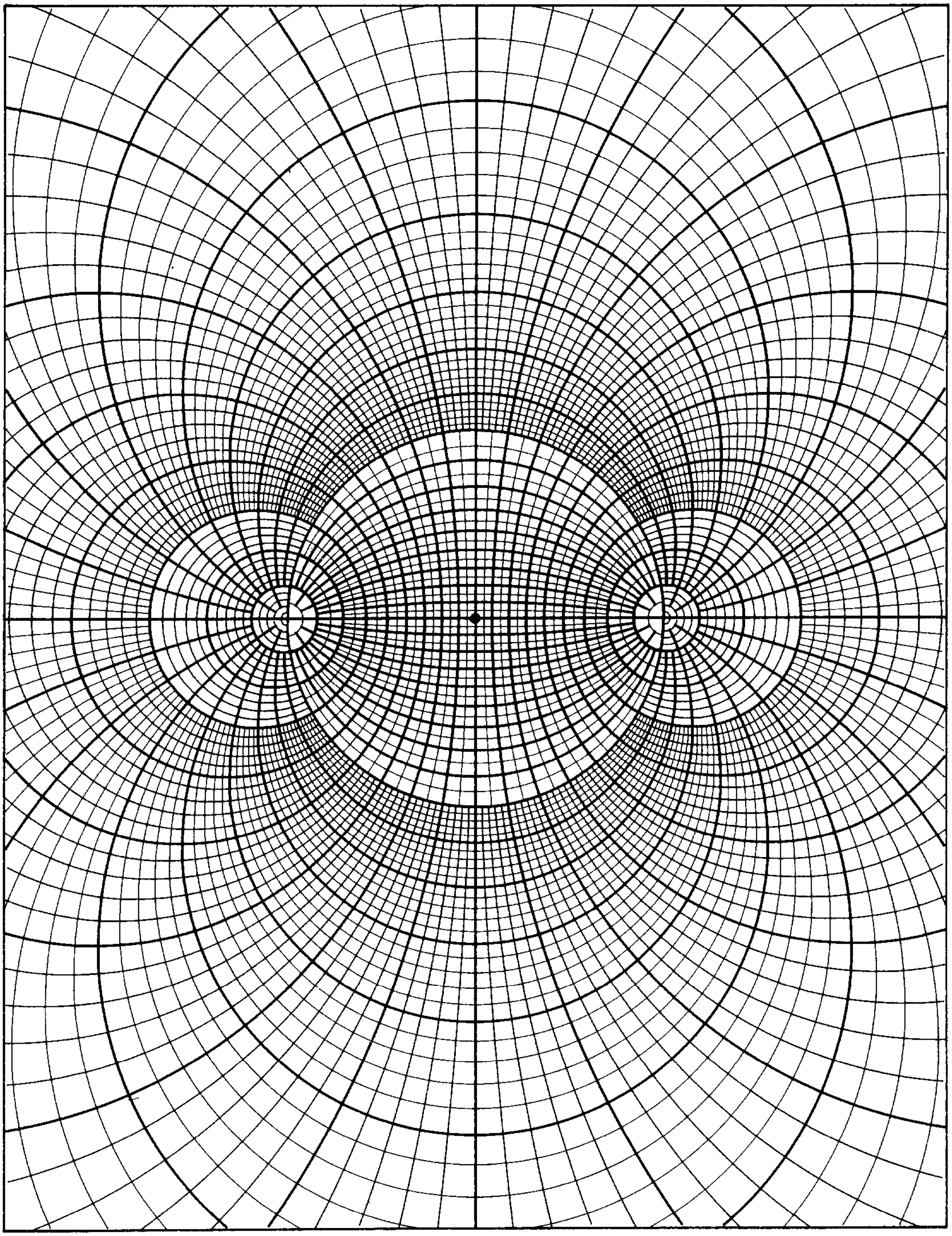

REFERENCES

Baecher, G. B., Lanny, N. A. & Einstein, N. H. (1977). Statistical description of rock properties and sampling. *Proc. 18th US Symp. Rock Mech.*, 5C1–8.

Barton, N. R. & Bandis S. C. (1983). Effects of block size on the shear behaviour of jointed rock. *Proc. 23rd US Symp. Rock Mech.*, 739–760.

Barton, N. R. & Choubey, V. (1977). The shear strength of rock joints in theory and practice. *Rock Mech.* **10,** 1–54.

Barton, C. C. & Larsen, E. (1985). Fractal geometry of two-dimensional fracture networks at Yucca Mountain, Southwestern Nevada. In *Fundamentals of rock joints*, pp. 77–84. Rotterdam: Balkema.

Chan, L. Y. & Goodman, R. E. (1983). Prediction of support requirements for hard rock excavations using key block theory and joint statistics. *Proc. 24th US Symp. Rock Mech.*, 557–576.

Crawford, A. & Bray, J. W. (1983). Influence of the in-situ stress field and joint stiffness on rock wedge stability in underground openings. *Can. Geotech. J.* **20,** 276–287.

Chern, J. & Wang, M. (1993). Computing 3-D key blocks delimited by joint traces on tunnel surfaces. *Int. J. Rock Mech. Min. Sci.* **30,** No. 7, 1599–1604.

de Freitas, M. H. & Watters, R. J. (1973). Some field examples of toppling failure. *Géotechnique* **23,** No. 4, 495–514.

Dershowitz, W., Lee, G., Geier, J., Hitchcock, S. & LaPointe, P. (1995). *User documentation.* FracMan Code version 2.42. Seattle: Golder Associates.

Goodman, R. E. (1976). *Methods of geological engineering in discontinuous rocks.* St Paul, Mn: West.

Goodman, R. E. (1989). *Introduction to rock mechanics*, 2nd edn. New York: Wiley.

Goodman, R. E. & Bray, J. W. (1977). Toppling of rock slopes. *Proceedings of specialty conference on rock engineering for foundation and slopes*, vol. 2, 201–234.

Goodman, R. E. & Scott, G. A. (1994). Rock mechanics dam safety studies for Seminoe arch dam. *Proc. 1st North Am. Rock Mech. Symp.*, 1051–1065.

Goodman, R. E. & Shi, G. H. (1985). *Block theory and its application to rock engineering.* Englewood Cliffs, NJ: Prentice-Hall.

Goodman, R. E., Shi, G. H. & Boyle, W. (1982). Calculation of support for hard, jointed rock using the keyblock principle. *Proc. 23rd US Symp. Rock Mech.*, 883–898.

Hatzor, Y. (1992). *Validation of block theory using field case histories.* PhD thesis, University of California.

Hatzor, Y. & Goodman, R. E. (1992a). Application of block theory and the critical key block concept to tunnelling: two case histories. *Proceedings of conference on fractured and jointed rock masses.* Rotterdam: Balkema.

Hatzor, Y. & Goodman, R. E. (1992b). Determination of the 'design block' for tunnel supports in highly jointed rock. In *Comprehensive rock engineering*, vol. 2. *Analysis and design methods* (ed. C. Fairhurst), 263–292.

Hoek, E. (1983). Strength of jointed rock masses. *Géotechnique* **33,** No. 3, 187–223.

Hoek, E. & Bray, J. W. (1981). *Rock slope engineering*, 3rd edn. London: IMM.

ISRM Commission on Standardization of Laboratory and Field Tests (1978). Suggested methods for the quantitative description of discontinuities in rock masses. *Int. J. Rock Mech. Min. Sci.* **15,** No, 6, 319–368.

John, K. W. (1968). Graphical stability analyses of slopes in jointed rock. *J. Soil Mech. Fdns Div. Am. Soc. Civ. Engrs* **94,** 497–526.

Karzulovic, A. L. (1988). *The use of keyblock theory in the design of linings and supports for tunnels.* PhD thesis, University of California.

Ke, T. C., Thapa, B. & Goodman, R. E. (1994). Stability analysis of a penstock slope. *Proc. 1st North Am. Rock Mech. Symp.*, 1109–1116. Rotterdam: Balkema.

Kuszmaul, J. (1992). *A probabilistic method to estimate key-block sizes in underground excavations.* PhD thesis, University of California.

Kuszmaul, J. & Goodman, R. E. (1992). An analytical model for estimating keyblock sizes in excavations in jointed rock masses. *Proceedings of international conference on fractured and jointed rock masses*, 26–33. Rotterdam: Balkema

Lindquist, E. S. & Goodman, R. E. (1994). Strength and deformation properties of a physical model melange. *Proc. 1st North Am. Rock Mech. Symp.*, 843–850. Rotterdam: Balkema.

Londe, P., Vigier, G. & Vormeringer, R. (1969). Stability of rock slopes. *J. Soil Mech. Fdns Div. Am. Soc. Civ. Engrs*, Part 1, **95,** 235–262.

Londe, P., Vigier, G. & Vormeringer, R. (1970). Stability of rock slopes. *J. Soil Mech. Fdns Div. Am. Soc. Civ. Engrs*, Part 2, **96,** 1411–1434.

McCullagh, P. & Lang, P. (1984). Stochastic models for rock instability in tunnels. *Jl R. Statist. Soc.*, Series B, **46,** No. 2, 344–352.

Maerz, N. H. & Germain, P. (1992). Block size determination around underground openings using simulations based on scanline mapping. *Proceedings of conference on fractured and jointed rock masses* **1,** 34–41. Rotterdam: Balkema.

Mauldon, M. (1990). Probability aspects of the removability and rotatability of tetrahedral blocks. *Int. J. Rock Mech. Min. Sci.* **27,** 303–307.

Mauldon, M. (1992a). *Rotational failure modes in jointed rock: a generalization of block theory.* PhD thesis, University of California.

Mauldon, M. (1992b). Relative probabilities of joint intersections. *Proc. 33rd US Symp. Rock Mech.*, 767–774.

Mauldon, M. (1995). Keyblock probabilities and size distributions: a first model for impersistent 2-d fractures. *Int. J. Rock Mech. Min. Sci.* **31,** No 2, 107–116.

Mauldon, M. & Goodman, R. E. (1990). Rotational kinematics and equilibrium of blocks in a rock mass. *Int. J. Rock Mech. Min. Sci.* **27,** No. 4, 291-304.

Mauldon, M. & Goodman, R. E. (1995). Vector analysis of keyblock rotations—kinematics, failure modes and stability. *J. Geotech. Div. Am. Soc. Civ. Engrs.*

Medley, E. & Goodman, R. E. (1994). Estimating the block volumetric proportions of melanges and similar block-in-matrix rocks (bimrocks). *Proc. 1st North Am. Rock Mech. Symp.*, 851–858. Rotterdam: Balkema.

Poisel, R., Steger, W. & Unterberger, W. (1991). The Malpasset Dam failure—comparison between continuum and discontinuum mechanics. *Proc. 7th Int. Congr. Rock Mech., Aachen*, 1893–1896. Aachen: International Society for Rock Mechanics.

Priest, S. D. (1985). *Hemispherical projection methods in rock mechanics*. London: George Allen & Unwin.

Priest, S. D. (1993a). The collection and analysis of discontinuity orientation data for engineering design, with examples. In *Comprehensive rock engineering*, vol. 3. *Rock testing and site characterization* (ed. J. Hudson), 167–192.

Priest, S. D. (1993b). *Discontinuity analysis for rock Engineering*. London: Chapman & Hall.

Rankine, W. J. M. (1874). *Songs and fables*, pp. 20–22. London: Macmillan.

Rengers, N. (1970). Influence of surface roughness on the friction properties of rock planes. *Proc. 2nd Congr. Int. Soc. Rock Mech., Belgrade* **1**, 229–234.

Shi, G. H. & Goodman, R. E. (1989). The key blocks of unrolled joint traces in developed maps of tunnel walls. *Int. J. Numer. Analyt. Meth. Geomech.* **13**, 131–158.

Shi, G. H., Goodman, R. E. & Tinucci, J. P. (1985). Application of block theory to simulated joint trace maps. *Proceedings of international symposium on fundamentals of rock joints, Bjorkliden*, 367–383. Rotterdam: Balkema.

Tanimoto, C. Morai, S., Matsumoto, T., Kishida, K. & Ando, T. (1992). Immediate image and its analysis of fractured and jointed rock masses through the borehole scanner. *Proceedings of conference on fractured and jointed rock masses*. Rotterdam: Balkema.

Terzaghi, K. (1960). Letter to J. Barry Cooke. 13 April.

Thapa, B. (1994). *Analysis of in-situ rock joint strength using downhole borehole scanner information*. PhD dissertation, University of California.

Warburton, P. M. (1987). Implications on keystone action for rock bolt support and block theory. *Int. J. Rock Mech. Min. Sci.* **24**, 283–290.

Ward, W. H. (1978). Ground supports for tunnels in weak rocks. *Géotechnique* **28**, No. 2, 135–170.

Wittke, W. (1965). Methods to analyze the stability of rock slopes with and without additional loading. *Rock mechanics and engineering geology*, supplement 2. Berlin: Springer-Verlag.

Wittke, W. (1984) *Felsmechanik*. Berlin: Springer-Verlag.

Yow, J. & Goodman, R. E. (1987). A ground reaction curve based on block theory. *Rock Mech. Rock Engng* **20**, 167–190.

VOTE OF THANKS

DR M. H. DE FREITAS, Imperial College of Science, Technology and Medicine

We have had the pleasure and the privilege of listening to a distinguished figure in the field of rock mechanics describe what amounts to his life's work. When a person of this eminence describes an achievement of this magnitude we should all listen, because behind such a story there is always another—just as rich—written to much the same music, certainly in the same key, but often sung to a different tune.

This is a story about a man who has successfully travelled a road on which many of us still journey—and because we are human and because we are curious it is always interesting to ask such a traveller what the road ahead is like.

This is a road that has no map—yet we know when we start our journey on it, and we know that we will recognize our destination when we see it, even if we cannot describe exactly what it is we are looking for. To help us on our journey we have the navigational instruments of science and engineering, and with these we can travel far. Yet on this road we are concerned to find ourselves passing fellow travellers who have just as good instruments as our own, and—what is even more alarming—we see travellers who, having tired of the task, have turned around and are now coming towards us. On this road the instruments of science and engineering are not sufficient for a successful journey: we also need vision, for this is the road on which we find the music-makers and the dreamers of dreams. Tonight we have heard the music and we have seen the product of dreams.

How long does such a journey take? This one took 30 years—not three years. Let that be an encouragement to those who fail and falter in the face of adversity—whose perserverance is put to the test. And let it also be a lesson to those of our sponsors who want their results in three years! Tonight we have seen the fruits of perseverance.

More important than all of this—because we are human—is the fact that few on this road complete their journey successfully without the aid of others. Richard Goodman has always been generous in acknowledging the help he has received from others and this increases a person's stature. More important than this is the effect it has on the fertility of the mind: a rich and fertile seedbed is created in which new ideas may take root and be nourished.

A seed came from the East; it came as an immigrant—an exile—an outcast from his own land and hardly able to speak the language of the country in which he sought asylum. Yet by great good fortune or providence, he came within the orbit of Richard Goodman who, by his work with others, could see the potential of this man. So it was that the theories of Gen Hua Shi enabled the seed of block theory to become a seedling, and the seedling to become a sapling, and the sapling to become a tree, and the tree to come to flower.

It is important to remember this and the role of partnership in human endeavour, especially in these times when so much emphasis is placed on individual achievement and single-author papers.

But what of the story? Did you detect an air of lyricism—a rhythm to the movement—a harmony to the argument? I did, and I can tell you why: although block theory is Richard Goodman's abiding interest—nay, his obsession—it is not his passion. His first love is music. This is probably why so many students like him. I have not yet met a single student who has not enjoyed being taught by Richard Goodman. He is clear, relaxed and to the point.

Tonight we have been his students and he has brought us these selfsame gifts. We thank him for them and for the inspiration that they bring, and most especially for being the 35th Rankine Lecturer.

Géotechnique 1995.45:383-423.